University of Stavanger

FACULTY OF SCIENCE AND TECHNOLOGY

MASTER'S THESIS

Study programme/specialisation: Petroleum Engineering/Reservoir Engineering	~~Spring~~/ Autumn semester, 2020. Open / ~~Confidential~~
Author: Abdullah Numan Tahmiscioglu	
Programme coordinator: Supervisor(s): Skule Strand Tina Puntervold Iván Darió Piñerez Torrijos	
Title of master's thesis: Optimized Smart Water Composition at Ekofisk Conditions-Oil Recovery at High Temperatures	
Credits: 30	
Keywords: Smart Water Wettability Alteration Ekofisk Chalk Carbonates	Number of pages: ……77…… + ~~supplemental material/other:~~ …… Stavanger, ……15.12.2020….. date/year

Title page for master's thesis
Faculty of Science and Technology

Master's Thesis

Optimized Smart Water Composition at Ekofisk Conditions

Oil Recovery at High Temperature

by

Abdullah Numan Tahmiscioğlu

December 15, 2020

Abstract

Seawater has been performing as a wettability modifier in chalk reservoirs and has been used for this purpose for a long time. This wettability alteration enhances microscopic then overall displacement efficiencies. Having the wettability-altering capability makes seawater possible to spontaneously imbibe into the chalk matrix and produce extra oil. Studies show that Ca^{+2}, SO_4^{-2}, and Mg^{+2}, potential determining ions, can be chemically active and desorbs the organic oil acids from the chalk mineral surface. This release of organic oil acids provides more water-wet wetting conditions for the reservoir mineral surfaces hence allowing more oil to be produced.

Smart Water is a designed injection brine that can modify reservoir wettability towards water wet. Knowing that seawater already functioning as a Smart Water in chalk reservoirs, to design the ideal Smart Water, seawater is considered as a base injection brine.
Smart Water for chalk needs to be abundant in Ca^{+2}, $SO_4^{-2,}$ and Mg^{+2} concentrations. It is also shown that low Na^+ and Cl^- concentrations help better displacement performance. The wettability alteration capability of Smart Water is directly related to reservoir temperature as well. Although slight Smart Water effect may be observed in low temperatures ~90 ºC, as temperature increases to ~130 ºC significant wettability alteration by Smart Water is observed.

In this thesis, finding composition, concentration, and stable equilibrium conditions for Smart Water is aimed. Stevns Klint chalk cores were used for their analogical importance to Ekofisk Field. Experiment temperature was also chosen as reservoir temperature of Ekofisk, 130 ºC to provide a better resemblance.
In total, four cores were cleaned with de-ionized water, restored 10% S_{wi} with sulfate-free formation water, and 90% S_{oi} with oil of AN:0.53 mgKOH/g. All cores aged for 14 days at 130 ºC. After a batch test, Smart Water is decided to be prepared as a 10 M $CaSO_4$ solution.

Spontaneous imbibition test with formation water recovered 30% of OOIP; seawater 58% of OOIP and $CaSO_4$ 30% of OOIP in secondary mode. In tertiary mode, $CaSO_4$ showed a slight wettability alteration and recovered an extra 8% of OOIP while seawater illustrated remarkable wettability modification and recovered 55% of OOIP after 30% of OOIP with formation water.

Seawater also experimented in tertiary mode and recovered 54% of OOIP after 30% of OOIP with $CaSO_4$ solution. This confirms the wettability alteration capabilities of seawater.

Acknowledgments

I would like to express my great appreciation to Professor Skule Strand and Professor Tina Puntervold for providing me this research opportunity and the invaluable guidance that they offered all the time.

I would like to address my sincere gratefulness to Dr. Iván Darió Piñerez Torrijos for offering his constant support, deep knowledge, and being a selfless teacher.

I also offer my profound gratitude to Tolgahan Aydıner, Bekir Aydemir, and my family for supporting my being without a rest.

I lastly would like to honor Alexandra Elbakyan for being a great motivation to me with her unshakeable stance.

.

List of Figures

List of Tables

Contents

Symbols and Abbreviations

A_{sample}	The area between SO_4^{-2} and SCN^- curves of the sample
$A_{heptane}$	The area between SO_4^{-2} and SCN^- curves completely water-wet reference core containing heptane
E	Total displacement efficiency, fraction
E_D	Microscopic displacement efficiency, fraction
E_v	Macroscopic displacement efficiency, fraction
g	Gravitational acceleration, 9.8 m/s^2
H	Height of the fluid column, m
I_o	Amott index for oil, fraction
I_w	Amott index for water, fraction
I_W^*	Modified Amott water index, fraction
k	Permeability, m^2
k_{rw}	Relative permeability of water, fraction
k_{ro}	Relative permeability of oil, fraction
L	Length of the capillary tube, m
M	Mobility ratio, fraction
J^*	Leverett dimensionless entry pressure
PV	Pore volume, ml
P_c	Capillary pressure, Pa
P_{NW}	The pressure of the non-wetting phase, Pa
P_W	The pressure of the wetting phase, Pa

r	Pore radius, m
S_{or}	Residual oil saturation, fraction
S_{wi}	Irreducible water saturation, fraction
S_{oi}	Initial oil saturation, fraction
S_{wc}	Connate water saturation, fraction
SI_C	OOIP% after spontaneous imbibition of water in the core to be evaluated, %
SI_{WWC}	OOIP% after spontaneous imbibition of water in the strongly water-wet core, %
u	Darcy Velocity, m/s
WI	Wettability index
w_{target}	the weight of the core with S_w=10%, g
w_{dry}	the weight of the dry core, g
ΔP_g	Pressure difference over the oil-water interface due to gravity, Pa
$\Delta\rho$	Difference in the density of the two phases, kg/m^3
ΔP	The pressure difference across the capillary tube, Pa
ΔS_{ws}	Water saturation change due to spontaneous imbibition of water, fraction
ΔS_{wf}	Water saturation change due to forced injection of water, fraction
ΔS_{os}	Water saturation change due to spontaneous imbibition of oil, fraction
ΔS_{of}	Water saturation change due to forced injection of oil, fraction
μ	Fluid Viscosity, Pa.s
μ_w	Water viscosity, Pa.s
μ_o	Oil viscosity, Pa.s
λ_w	Mobility of water, m^2/ Pa.s

λ_o	Mobility of oil, m^2/ Pa.s
λ_D	Mobility of the displacing fluid, m^2/ Pa.s
λ_d	Mobility of the displaced fluid, m^2/ Pa.s
$\frac{dP}{dx}$	Pressure gradient, Pa/m,
σ	Interfacial tension, N/m
φ	Porosity, fraction
σ	Interfacial tension between wetting and non-wetting phase, N/m
θ	Contact angle, degree
υ_{ave}	Average flow velocity in the capillary tube, m/s
r	Radius of the capillary tube, m
υ_{o}	Velocity, m/s
σ_{ow}	Surface tension between oil and water, mN/m
σ_{os}	Oil-solid interfacial tension, mN/m
σ_{ws}	Water-solid interfacial tension, mN/m
ρ_{VB0S}	The density of the VB0S Brine, 1.0224 g/cm^3

1 Introduction

In a world that energy demand increases historically, petroleum still holds its economically important yet environmentally controversial place on the energy supply behalf.

Petroleum extraction has never been uncostly. Furthermore, advanced improvements in technology that are used and extreme conditions that new fields are being sought, keep supporting the high cost of new explorations. Consequently, producing proven reserves more efficiently is getting more attention than ever. Increasing oil recovery in proven reserves is the essential way to accomplish that.

Half of the world's oil rests in carbonate reservoirs. Due to their special nature, carbonate reservoirs tend to have high residual oil saturation in fractured porous systems that cannot be produced easily with primal yet conventional recovery techniques.
Just because of this, as a chemical enhanced oil recovery technique, Smart Water, has been researched carefully, observed, and experimented neatly.

In this master thesis research study, Smart Water has been investigated experimentally to answer some questions risen and confirm or refute some of the answers given in the past.

2 Objective

This thesis study primarily aims to research an injection brine, Smart Water, that shows a wettability alteration effect for chalk carbonates at 130 ºC and compare its oil recovery performance to the oil recovery performance of seawater for the same conditions.

The study also targets to find the ion composition and concentrations of the Smart Water that does not cause any precipitation in the pore water-rock-brine system and does function as a wettability modifier as a Smart Water is supposed to function.

Moreover, the study interests the oil recovery performance of the Smart Water and seawater in both secondary and tertiary modes after formation water.

Finally, the thesis aims to compare the oil recovery performance of Smart Water in the secondary mode after seawater; and the oil recovery performance of seawater in the secondary mode after Smart Water and analyze any possible wettability alteration.

3 Theory

3.1 Carbonate Reservoirs

Carbonate rocks are sedimentary rocks that are made mostly of carbonate minerals. These carbonate minerals are originated from calcareous organisms and animal debris. Due to the diversity of composition, it is useful to classify carbonate minerals so that elemental compositions show. Calcite ($CaCO_3$), Siderite ($FeCO_3$), Magnesite ($MgCO_3$), Dolomite ($CaMgCO_3$) and Ankerite ($CaFe(CO_3)_2$) are the carbonate minerals that make different carbonate rocks (Puntervold, 2008; Puntervold et al., 2008). For instance, limestone is classified as carbonate rock with %50 or more Calcite minerals while carbonate rock with %50 or more dolomite minerals is classified as dolomite.

Carbonate rocks, together with other necessary elements and processes, may constitute carbonate reservoirs and may host hydrocarbons. The carbonate reservoirs hold approximately 50% of petroleum reserves Treiber and Owens (1972).

3.2 Oil Recovery in Carbonate Rocks

Oil production is conventionally being executed under three stages, primary recovery, secondary recovery, and tertiary recovery. Primary recovery is the stage that the reservoir is produced with the energy stored in it. This energy can be one or combinations of solution gas drive, gas cap drive, gravity drive, rock expansion, aquifer expansion, or fluid expansion (Green & Willhite, 1998).

Secondary recovery is considered as supporting reservoir pressure against declining as production goes on. This support is typically in the practice of water and/or gas injection. Different fluids are being injected from injection wells to displace oil towards the production wells while supporting the reservoir pressure (Green & Willhite, 1998). In the secondary recovery stage, the average hydrocarbon recoveries range between 20-40% of the original oil in place (Muggeridge et al., 2014).

The tertiary recovery term is used to cover all recovery enhancement techniques that can be designed and performed in addition to secondary recovery methods. Although primary, secondary, and tertiary terms imply a sequential order due to their conventional applications,

these stages are not necessarily in order. For instance, a secondary recovery method of water flooding can be performed starting from the first day of production. To clarify the misconception among the terms, enhanced oil recovery, EOR term is being more used and accepted by the industry (Green & Willhite, 1998) and can be studied under categories of chemical methods, gas EOR methods, thermal methods, and emerging new methods.

3.3 Enhanced Oil Recovery

EOR focuses on extracting more oil from already existing oil fields that experience production declines. Being working on already existing fields gives EOR the chance to save a substantial amount of capital from exploration expenditures. In a world that oil has a 31.6% share of the total global energy supply as a source (IEA,2018), EOR still holds its important place in an industry that is in decline in discovering new giant oil fields (Cook, 2013).
Over decades, although people from diverse backgrounds, suggested EOR solutions from a different point of view, EOR methods happen to aim at least one of mobility ratio reduction, interfacial tension reduction, and wettability alteration principles to increase oil recovery.

Table 3.1 classifies these EOR methods under four categories (Torrijos et al., 2017).

Table 3.1 Classification of EOR methods

Chemical Methods	Surfactant Flooding Polymer Flooding Alkaline Flooding Alkaline-Surfactant-Polymer (ASP) Flooding Gels for Water Diversion/Shut-off Solvent Flooding
Gas EOR Methods	Hydrocarbon Injection (Miscible/Immiscible) CO_2 Flooding (Miscible/Immiscible) Nitrogen Flooding Flue Gas Injection (Miscible/Immiscible) Water Alternating Gas (WAG)
Thermal Methods	Steam Flooding Cycle Steam Stimulation In-situ Combustion

Thermal Methods	Hot Water Flooding Steam Assisted Gravity Drainage
Emerging EOR Methods	Smart Water Low Salinity Waterflooding Carbonated Waterflooding Microbial EOR Enzymatic EOR Electromagnetic Heating Surface Mining and Extraction Nano Particles

3.4 Displacement Efficiencies and Forces

3.4.1 Microscopic and Macroscopic Displacement

The total displacement efficiency is defined as the product of microscopic and macroscopic displacement efficiencies. The total displacement efficiency is defined as follows,

$$E = E_D E_v \qquad 3.1$$

Where

E Total displacement efficiency, fraction

E_D Microscopic displacement efficiency, fraction

E_v Macroscopic displacement efficiency, fraction

Equation 3.1 summarizes that the closer E gets to the 1, the higher the displacement efficiency of oil is. In Equation 3.1, E_D represents mobilization of oil in pore scale and directly related to S_{or} while E_v represents how well displacement progresses through the reservoir, volumetrically.

EOR processes are often about decreasing the S_{or} then increasing E_D.While S_{or} is dictated by chemical and physical relations between oil, water, and rock; IFT and wettability alteration

emerge as important concepts to decrease S_{or} then increase E_D. Equation 3.2 shows how E_D and S_{or} relates.

$$E_D = \frac{S_{oi} - S_{or}}{S_{oi}} \qquad 3.2$$

Where

E_D Microscopic displacement efficiency, fraction

S_{oi} Initial oil saturation, fraction

S_{or} Residual oil saturation, fraction

Unlike E_D, E_v is resulted from macroscopic factors like reservoir geometry and structure, viscosity ratio, and density differences of displacing and displaced fluids. An unfavorable reservoir geometry, high density, and viscosity differences cause high mobility ratios and poor flooding performance hence early water breakthrough. But ideally, E_D is being studied to be increased by creating a uniform flood front with a low mobility ratio to have a late water breakthrough.

3.4.2 Fluid Flow in Porous Media

Darcy's fluid flow law constructs the relation between porous medium and fluid that flows through it. Darcy's law, Equation 3.3 defines the permeability of the porous medium by measuring the flow rate and the pressure difference between flow inlet and outlet.

$$u = -\frac{k}{\mu}\frac{dP}{dx} \qquad 3.3$$

Where

u Darcy Velocity, m/s

k Permeability, m^2

μ Fluid Viscosity, Pa.s

$\frac{dP}{dx}$ Pressure gradient, Pa/m,

In a waterflooding case, water is displacing and oil is being displaced, viscosities of the fluids and the wettability determine the mobility of the phases in the presence of the other phase (Torrijos et al., 2017). Mobility of water and oil phases are defined as follows in Equation 3.4 and 3.5

$$\lambda_W = (\frac{k_{rw}}{\mu_w})_{S_{or}} \quad 3.4$$

$$\lambda_O = (\frac{k_{ro}}{\mu_o})_{S_{wi}} \quad 3.5$$

Where

λ_w Mobility of water, m^2/ Pa.s

λ_o Mobility of oil, m^2/ Pa.s

k_{rw} Relative permeability of water, fraction

μ_w Water viscosity, Pa.s

k_{ro} Relative permeability of oil, fraction

μ_o Oil viscosity, Pa.s

S_{or} Residual oil saturation, fraction

S_{wi} Initial water saturation, fraction

In addition to mobilities, the ratio of phase mobilities becomes practical to qualify how phases move together in co-existence with each other.

The mobility ratio, M is defined as follows.

$$M = \frac{\lambda_D}{\lambda_d} = \frac{\lambda_w}{\lambda_o} = \frac{(\frac{k_{rw}}{\mu_w})_{S_{or}}}{(\frac{k_{ro}}{\mu_o})_{S_{wi}}} \quad 3.6$$

Where

M Mobility ratio, fraction

λ_D Mobility of the displacing fluid, m^2/ Pa.s

λ_d Mobility of the displaced fluid, m^2/ Pa.s

λ_w Mobility of water, m^2/ Pa.s

λ_o Mobility of oil, m^2/ Pa.s

k_{rw} Relative permeability of water, fraction

μ_w Water viscosity, Pa.s

k_{ro} Relative permeability of oil, fraction

μ_o Oil viscosity, Pa.s

S_{or} Residual oil saturation, fraction

S_{wi} Initial water saturation, fraction

In fractured carbonate reservoirs, spontaneous imbibition rules the recovery mechanism, and the wettability of the mineral surface determines most of recovery efficiency. In an oil-wet system, due to having the capillary pressure working against the oil displacement, imbibing fluid needs to overcome a capillary entry pressure to the matrix. The Leverett J-function claims to calculate this capillary entry pressure as follows

$$P_c = \sigma\sqrt{\frac{\varphi}{k}}\,J^* \qquad 3.7$$

Where

P_c Capillary pressure, Pa

σ Interfacial tension, N/m

φ Porosity, fraction

J^* Leverett dimensionless entry pressure ($J^* \approx 0.25$ for completely water wet and)

3.4.3 Capillary Forces

Capillary pressure is the pressure difference between two sides of the interphase of two immiscible fluids. (Green & Willhite, 1998). Capillary force is the force determining the fluid distribution and displacement in a reservoir system. Capillary forces also are affected by geometry and dimensions of pore throats, wettability, and interfacial tension. Capillary forces can work in favor of oil displacement in a fractured reservoir while in a non-fractured reservoir it can cause oil trapping and increase residual oil saturation. Capillary pressure is defined as follows.

$$P_c = P_{NW} - P_W = \frac{2\sigma cos\theta}{r} \qquad 3.8$$

Where

P_c, Capillary pressure, Pa

P_{NW}, The pressure of the non-wetting phase, Pa

P_W, The pressure of the wetting phase, Pa

σ, Interfacial tension between wetting and non-wetting phase, N/m

θ, Contact angle, degree

r, Pore radius, m

3.4.4 Gravity Forces

Gravity forces are the gravitational forces that are exerted on fluids. In the case of having large density differences between fluids, and low oil-water interfacial tension conditions, gravity forces become significant. Gravity force difference can be calculated as follows

$$\Delta P_g = \Delta \rho g H \qquad 3.9$$

Where

ΔP_g Pressure difference over the oil-water interface due to gravity, Pa

$\Delta\rho$ Density difference of the two phases, kg/m^3

g Gravitational acceleration, 9.8 m/s^2

H Height of the fluid column, m

3.4.5 Viscous Forces

During fluid flow in porous media, flow faces resistance. The resistance depends on the properties of the porous medium and the flow itself. The viscous forces are reflected as a pressure drop (Green & Willhite, 1998). For the sake of simplification, the porous medium is regarded as a pack of many parallel capillary tubes that laminar flow happens to be in them. Pressure drop due to viscous forces is calculated as in Equation 3.10.

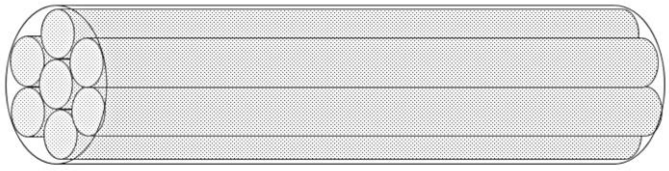

Figure 3.1 The simplified porous medium as a pack of parallel capillary tubes (Lindanger, 2019)

$$\Delta P = -\frac{8\mu L v_{ave}}{r^2 g_c} \qquad 3.10$$

Where

ΔP The pressure difference across the capillary tube, Pa

μ Viscosity, Pa.s

L Length of the capillary tube, m

v_{ave} Average flow velocity in the capillary tube, m/s

r Radius of the capillary tube, m

3.4.6 Capillary Number

Capillary number, N_c is the dimensionless ratio of viscous forces to capillary forces that exist in the porous medium. If viscous forces dominate the porous flow, the capillary number increases leading the residual oil saturation to decrease. On the other hand, if capillary forces dictate the porous flow, the capillary number appears to be smaller. As the capillary number gets smaller, it might indicate that oil possibly can get capillary trapped and increase the residual oil saturation. The capillary number is calculated as in Equation 3.11 (Moore & Slobod, 1955)

$$N_c = \frac{\mu_w v_o}{\sigma_{ow} cos\theta} \qquad 3.11$$

Where

μ_w Water viscosity, mPa.s

v_o Velocity, m/s

σ_{ow} Surface tension between oil and water, mN/m

θ Contact angle, degree

3.5 Wettability

Wettability is described as being the tendency of a fluid to spread on a solid rock surface in the presence of other immiscible fluids. It is known to be one of the major factors affecting multiphase flow properties and fluid distribution in porous media (Craig, 1971; Kovscek et al., 1992). Aging, temperature, and the surface charge affect the wettability behavior of a mineral surface to a certain fluid (Strand, 2005). Wettability is also known for changing oil displacement efficiencies by affecting relative permeability curves, capillary pressure, and finally residual oil saturation (Anderson, 2013). Hence altering the wettability in a way that oil displacement efficiencies improve, is of great interest for those who aim to improve oil recovery.

3.5.1 Wettability in Porous Media

For the scope of petroleum studies, in the co-existence of two immiscible fluids, oil, and water; wettability is conceptualized between two extremes of being strongly oil-wet and being strongly water-wet. All porous sedimentary medium is known to be originally water-wet due to lack of oil presence. After oil migrates into the sedimentary medium, factors that determine

the wettability state change and reach an equilibrium at which the initial wettability state of the reservoir establishes.

The wettability behavior of the mineral surface is not necessarily homogenous for all across the reservoir. The rock happens to have a heterogeneous wettability if specific mineral surface regions have a specific affinity to water or oil. In this fractional wetting condition, rock is considered as partially oil-wet and partially water-wet for the different parts of the rock surface.

In a strongly oil-wet porous system, the oil covers most of the rock surface creating a thin oil film on the mineral surface of the rock. Oil fills small pore spaces and forces water to be in the middle of the larger pores. During water flooding, as shown in Figure 3.2(a) water does not reach these small pores and flows mainly through the larger pores. This causes poor oil displacement efficiencies and high residual oil saturation.

Contrarily, in a strongly water-wet porous system, water covers most of the rock surface and fills small pores, leaving oil in the larger pores. During water flooding, oil volumes in the larger pores might get trapped in Figure 3.2(b) (Strand, 2005).

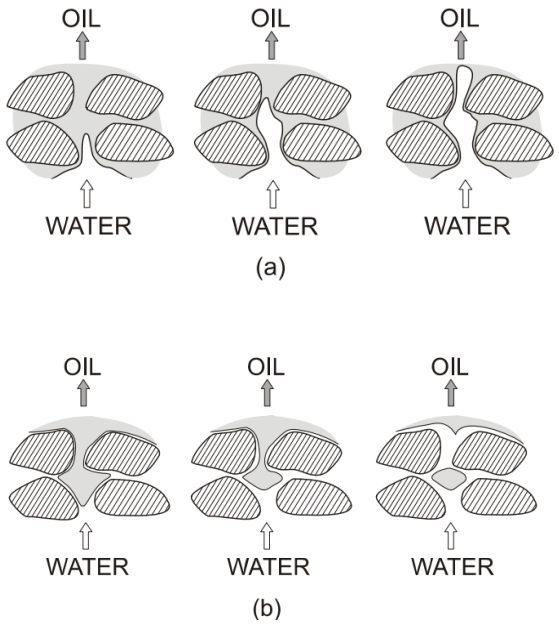

Figure 3.2 Displacement of oil by waterflooding for (a) oil-wet, and (b) water-wet mineral surfaces (Strand, 2005)

Among many factors determining the wettability profile of a porous system, crude oil components and mineral composition can be named as two of the most important factors.

Asphaltene and resin groups in crude oil are known to be affecting wetting due to the polar molecules in them that show acidic or basic character by nature (Anderson, 1986; Buckley, 1996).

Mineral composition interaction with polar components differs from sandstone to carbonate rocks. (Buckley & Liu, 1998; Denekas et al., 1959). The carbonate mineral surface is generally positively charged below pH 8-9 and attracts negatively charged surface-active ions. If the mineral surface adsorbs negatively charged acidic oil components it becomes more oil-wet (Pierre et al., 1990). Sandstone mineral surface, on the other hand, charged negatively above pH 2 (Menezes et al., 1989) and adsorbs basic oil components and positively charged surface-active ions. (Cuiec, 1984; Kowalewski et al., 2003; Torsæter & Silseth, 1985). If basic oil components get adsorbed to sandstone mineral surface, it becomes more oil-wet.

3.5.2 Effects of Wettability

Understanding wettability in a porous system is important due to its critical effects on multiphase flow, fluid distribution, and phase trapping. Wetting is also found in direct relation to the capillary pressure, relative permeability, electrical properties, irreducible saturation, and many EOR processes (Strand, 2005).

3.5.3 Wettability in Carbonates

Most of the reservoir minerals are originally strongly water-wet due to the absence of polar components in the porous system. However, with oil intrusion along with the other factors, the wettability profile changes to set the initial wettability of the rock mineral to oil or water. Due to their mineral characteristics, carbonate rocks tend to be neutral to oil-wet (Chilingar & Yen, 1983; Treiber & Owens, 1972). Along with being oil-wet, carbonate reservoirs are also known to be challenging due to their fractured nature. In an oil-wet reservoir, high permeable fracture networks dominate fluid flow through the medium while tight matrix blocks are flow-wise partially isolated, and keeping the oil within them with strong capillary forces. This results in the injection water not being able to imbibe sufficiently to the oil-bearing rock matrix. In these reservoirs, water injection does not function as efficiently as it does so in water-wet reservoir systems. (Strand, 2005).

Wettability is being determined depending on many factors and parameters (Standnes, 2001). Functional polar components in the crude oil, and solubility of polar oil components in the water, surface charge and mineral composition of the rock (Anderson, 2013; Buckley et al., 2013), brine salinity, and concentration of potential determining ions (Buckley, 1996),

capillary pressure and thin-film forces, disjoining pressure (Hirasaki, 1991), the ability of the oil to stabilize heavy components (Al-Maamari & Buckley, 2013), temperature, pressure (Al-Maamari & Buckley, 2013), initial water saturation (Jadhunandan & Morrow, 2013) are major factors and parameters that determine the wettability state.

3.6 Wettability Measurement

Being such an important parameter for petroleum reservoirs, makes wettability measurement crucial as well. There are many different approaches developed over the years to measure wettability. Three of them are presented as follows.

3.6.1 Contact Angle Measurement

The main approach to determine the wetting state and quantify it is by contact angle measurement (Yuan & Lee, 2013). In a model wetting environment, rock is cut, the rock surface is smoothened then exposed to two immiscible fluids of interest. After fluids settle on the rock surface, the contact angle is measured through the denser phase as in Figure 3.3.

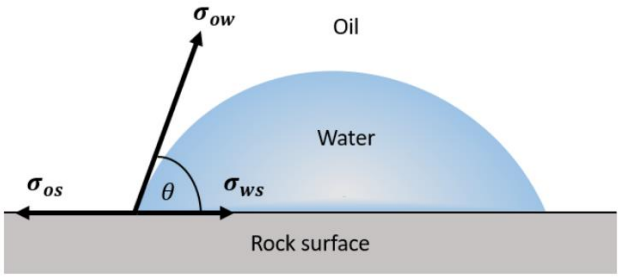

Figure 3.3 Contact angle measurement (Lindanger, 2019)

The static equilibrium in Figure 3.3 can be defined by Young's equation, Equation 3.12 which was developed on a thermodynamic basis stated by Gibbs (Letellier et al., 2007).

$$\sigma_{os} = \sigma_{ws} + \sigma_{ow} \cos\theta \qquad 3.12$$

Where

σ_{os} Oil-solid interfacial tension, mN/m

σ_{ws} Water-solid interfacial tension, mN/m

σ_{ow} Oil-Water interfacial tension, mN/m

θ Contact angle measured through the denser phase, degree

Wettability states that can be interpreted by contact angle measurement ranges are presented in Table 3.2.

Table 3.2 Wettability states for the range of contact angles

Contact angle, degree	Wettability
0-30	Strongly water wet
30-90	Water wet
90	Neutral wet
90-150	Oil wet
150-180	Strongly oil-wet

Although contact angle theory is fundamental to understand wettability, contact angle measured on model surfaces is not representative to practice it for real reservoir rock oil-brine systems. Moreover, contact angle measurement is not easily applicable in reservoir rock pore space due to large fluid droplets that will not fit into nanometer or micrometer diameter pores. Also analyzing images taken to measure contact angle is not applicable even by using micro CT. These problems bring the need for other methods to measure wettability.

3.6.2 Amott Harvey Method

Amott proposed a quantitative method to calculate the average wettability of a core by measuring water saturation and capillary pressure through five imbibition and drainage processes (Amott, 1959).

As presented in Figure 3.4, the measurement starts with the primary drainage of oil which is oil injection into a core (arrow 1) that is entirely saturated with water. In the beginning, oil enters through the widest pores at the injection inlet after overcoming the capillary entry pressure and then oil finds a connected pathway through the system with an invasion percolation like flow. As oil occupies smaller pores it needs to pass through smaller pore throats hence faces larger capillary pressure. At the end of the injection, the core still has some water (S_{wc}) that cannot be displaced by oil injection.

Measurement continues with spontaneous imbibition of water (arrow 2) where water fills the water wet regions of the pore space preferentially till capillary pressure becomes zero. Then forced water injection (arrow 3) occurs where water displaces the oil until water saturation becomes $1\text{-}S_{or}$. Later, oil spontaneously imbibe (arrow 4) into the core, displaces the water till capillary pressure reaches zero. Lastly, secondary drainage (arrow 5) takes place and oil displaces water till water saturation becomes $S_{wc.}$ Along with all the imbibition and drainage processes, water saturation values are recorded where capillary pressure becomes zero. Hence Amott index for water, I_w and oil, I_o are defined and calculated as in Equation 3.13 and Equation 3.14.

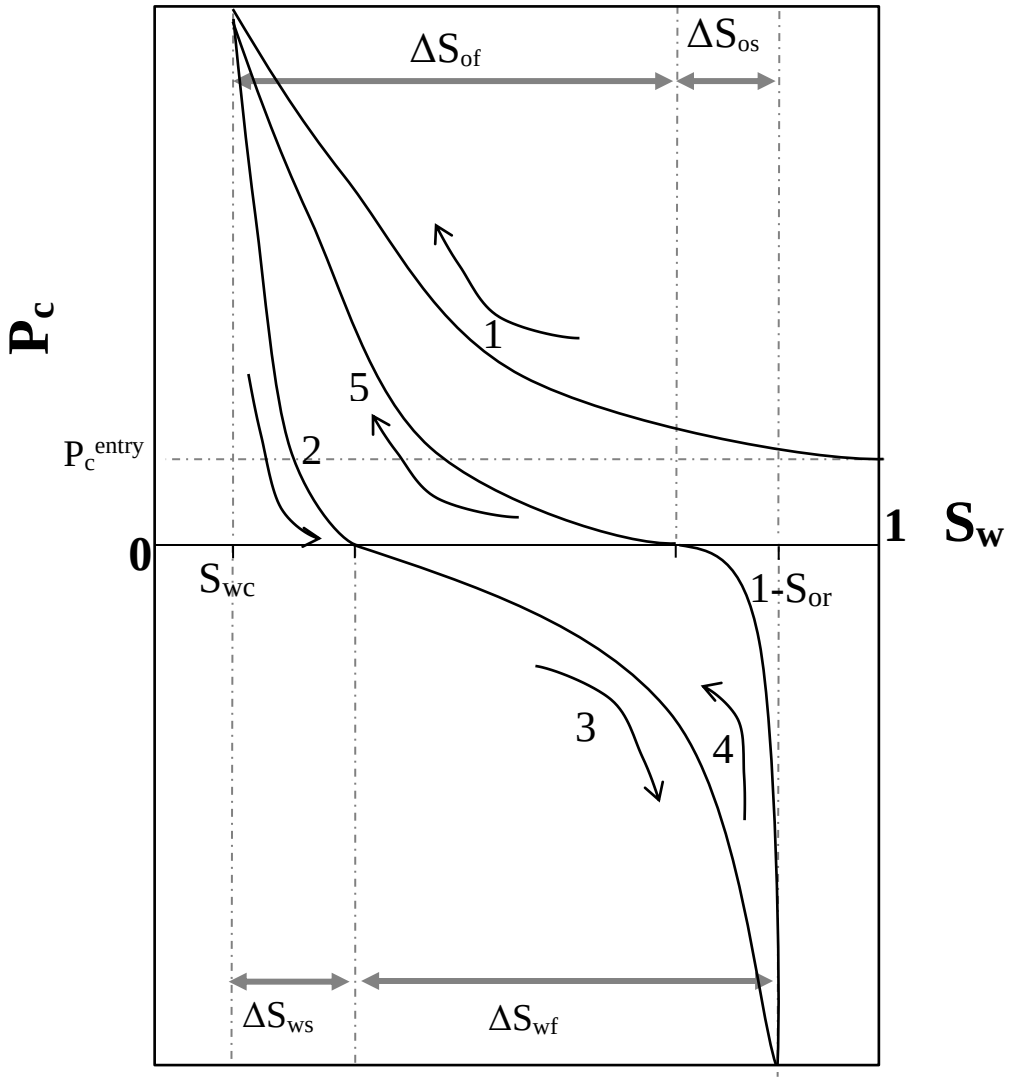

Figure 3.4 Capillary pressure curves for Amott and Amott-Harvey Methods

$$I_w = \frac{\Delta S_{ws}}{\Delta S_{ws} + \Delta S_{wf}} \qquad 3.13$$

Where

I_w Amott index for water, fraction

ΔS_{ws} Water saturation change due to spontaneous imbibition of water, fraction

ΔS_{wf} Water saturation change due to forced injection of water, fraction

$$I_o = \frac{\Delta S_{os}}{\Delta S_{os} + \Delta S_{of}} \qquad 3.14$$

Where

I_o Amott index for oil, fraction

ΔS_{os} Water saturation change due to spontaneous imbibition of oil, fraction

ΔS_{of} Water saturation change due to forced injection of oil, fraction

S_{wc} Connate water saturation, fraction

S_{or} Residual oil saturation, fraction

The Amott Harvey Index is defined as in Equation 3.15 using Amott indices as defined above

$$I_{AH} = I_o - I_w \qquad 3.15$$

The Amott Harvey index ranges between -1 and 1 for the extremes of wettability states. Ranges for the Amott Harvey index are presented as follows (Cuiec, 1984).

Table 3.3 Amott Harvey index for different wetting states

$\mathbf{I_{AH}}$	**Wettability state**
$-1 \leq I_{AH} \leq -0.3$	Oil-wet
$-0.3 < I_{AH} < 0.3$	Mixed-wet
$0.3 \leq I_{AH} \leq 1$	Water-wet

3.6.3 Spontaneous Imbibition

Spontaneous imbibition is a simplistic and qualitative way of measuring wettability in comparison to a reference wetting, preferentially a strongly water-wet or a strongly oil-wet core. The application starts with a core with initial water saturation. The core is immersed in imbibing water. The produced oil volume is recorded as a function of time. The production rate is compared to a strongly water-wet reference core. If spontaneous imbibition of water does not occur then similarly, the core at residual oil saturation is immersed in imbibing oil, and produced water volume is recorded as a function of time. The production rate is compared to a reference strongly oil-wet core.

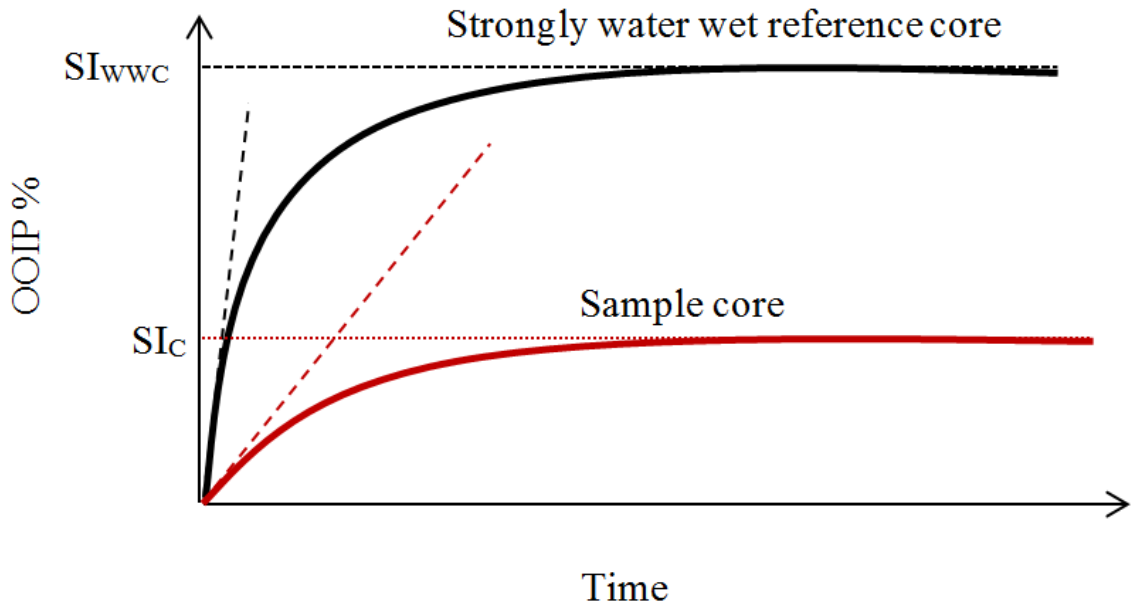

Figure 3.5 Illustration of spontaneous imbibition of water

The degree of wettability compare to the reference core can be calculated by using the modified Amott water index as follows (Zhou et al., 1996).

$$I_W^* = \frac{\mathrm{SI_C}}{\mathrm{SI_{WWC}}} \qquad 3.16$$

Where

I_W^* Modified Amott water index, fraction

$\mathrm{SI_C}$ OOIP% after spontaneous imbibition of water in the core to be evaluated, %

$\mathrm{SI_{WWC}}$ OOIP% after spontaneous imbibition of water in the strongly water-wet core, %

In the interpretation of the modified Amott index results, I_W^*=1 indicates evaluation core is strongly water wet, while $I_W^* = 0$ hints that the evaluation core is neutral wet.

3.6.4 Chromatographic Wettability Test

A recent method has been proposed to measure the wettability of carbonate cores (Skule Strand et al., 2006). Unlike Amott's and spontaneous imbibition methods, the chromatographic wettability test focuses on mineral surface chemistry. The method relies on water flooding a core with known concentrations of SO_4^{-2} and SCN^-. Flooding effluents are analyzed later to see SO_4^{-2} and SCN^- concentration. The method is designed upon SO_4^{-2} ions are getting adsorbed on water-wet carbonate mineral surfaces where SCN^- being a non-absorbing ion as a tracer.

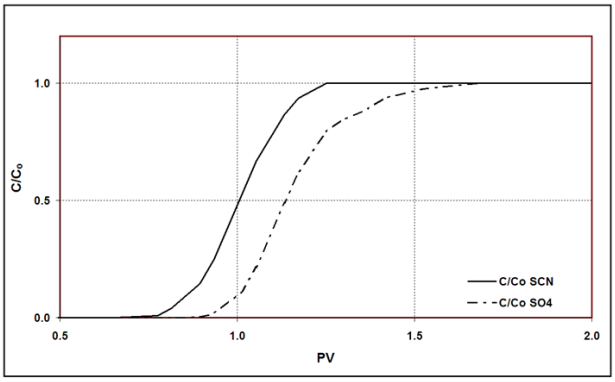

Figure 3.6 Typical chromatography wettability result for a water-wet carbonate core

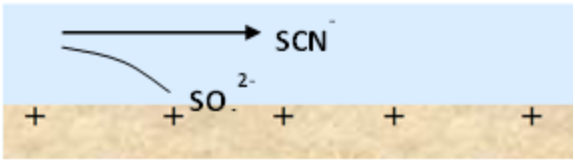

Figure 3.7 Illustration of SCN^- and SO_4^{-2} ions around water-wet carbonate mineral surface.

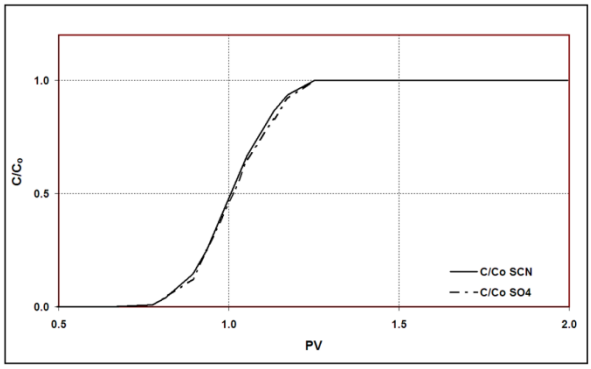

Figure 3.8 Typical chromatography wettability result for an oil-wet carbonate core

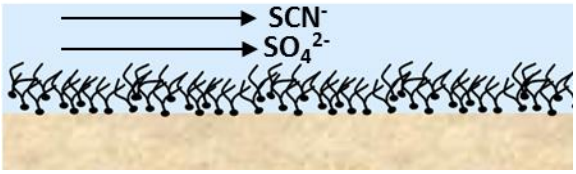

Figure 3.9 Illustration of SCN^- and SO_4^{-2} ions around the oil-wet carbonate mineral surface.

The wettability index is calculated as follows regarding the ratio of the area between SO_4^{-2} and SCN^- curves of the tested sample. The area representing the sample core is compared to the water-wet reference core containing the only heptane. The degree of wetness is determined as follows.

$$WI = \frac{A_{sample}}{A_{heptane}} \qquad 3.17$$

Where

WI Wettability index

A_{sample} The area between SO_4^{-2} and SCN^- curves of the sample

$A_{heptane}$ The area between SO_4^{-2} and SCN^- curves completely water-wet reference core containing heptane

In interpretation,

$WI_{new} = 1.0$ represents a completely water-wet system

$WI_{new} = 0.5$ represents an intermediate water-wet system

$WI_{new} = 0.0$ represents a completely oil-wet system.

4 Water-Based EOR in Carbonates

4.1 Waterflooding

Waterflooding has been widely accepted and practiced as a recovery technique for a long time to provide pressure support to the reservoirs to slow down the production decline. Being studied and applied vastly made waterflooding possible to investigate its strength and weaknesses. For example, it is shown that (Alvarez & Sawatzky, 2013) waterflooding is not as efficient for heavy oil reservoirs as it is efficient for light oil reservoirs. It is due to the low macroscopic displacement efficiency that occurs between the water and heavy oil phase. On the other hand, Wade studies (Wade, 1971) 53 waterflooding cases statistically and shows that waterflooding results in an average oil recovery of 23.3% off total pore volume while the average primary oil recovery was 9.4%. This shows that oil recovery can be largely increased by applying waterflooding.

In addition to efficiencies, drawbacks that waterflooding designs might face also are studied and seen that formation water-injection water compatibilities, scaling issues, corrosion control, sand production troubles are some of the problems to be considered prior to the waterflooding planning.

Moreover, waterflooding is researched also concerning injection water composition after seeing the results that not all water sources lead to similar oil displacement results. Hence, different injection waters have been studied to see their displacement efficiencies and finally recovery results in flooding cases.

In carbonate reservoirs, seawater has been used in its availability as injection water and a vast improvement in oil displacement is observed. Being a natural displacement enhancer in carbonate reservoirs attracts lots of research attention to seawater and its composition.

4.2 Wettability Alteration in Carbonate by Modifying the Ionic Composition of Water

After being accepted and used as proper injection water for carbonates, seawater was researched regarding the mechanism that affects oil displacement. Knowing that seawater does not provide any significant macroscopic displacement efficiency improvement on its

own, researchers focused on properties of seawater that affect microscopic displacement efficiency, namely the wettability of the rock-brine-oil system.

Studies show that (S. Strand et al., 2006; Zhang & Austad, 2006; Zhang et al., 2007a) wetting state in the porous medium can be enhanced by flooding with water that ionic composition of which is selected or modified in the favor of flooding efficiencies. In fractured chalk reservoirs, seawater was discovered to be wettability-altering flooding water that improves oil displacement (Strand et al., 2008). In Figure 4.1, Strand et al. experiment sequential spontaneous imbibition and viscous flooding with two equally restored chalk cores at 120 ºC. The Core C#6 was initially spontaneously imbibed with FW and recovery resulted in around 12% of OOIP. Next, SI brine changed from FW to SW and resulted in 18% of OOIP extra oil recovery. Having this recovery improvement shows that SW is a valid wettability modifier and acts as a Smart Water for chalk at 120 ºC.

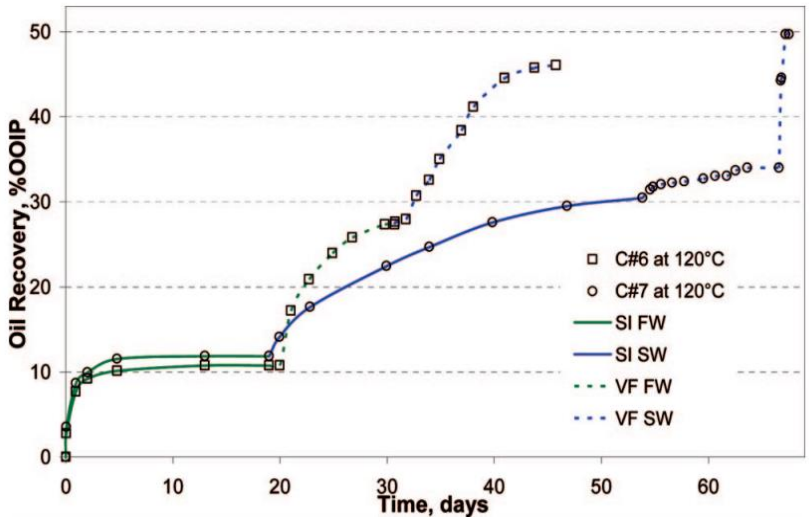

Figure 4.1 Oil recovery at 120 ºC by successive spontaneous imbibition and forced displacement (Strand et al., 2008)

Zhang also studied (Zhang et al., 2007a) the similar effect by using equally restored chalk cores, and showed how different injection brines affect the oil displacement differently. In the study, as a base case FW with no sulfate was spontaneously imbibed into a core and around 18% of OOIP was recovered. To see the SW effect on the oil recovery, SW was used in the spontaneous imbibition experiment and resulted in around 38 % of OOIP, giving an extra 20 % of OOIP compare to FW. This shows how SW acts as a Smart Water in chalk cores at 90 ºC and modifies wettability (Figure 4.2).

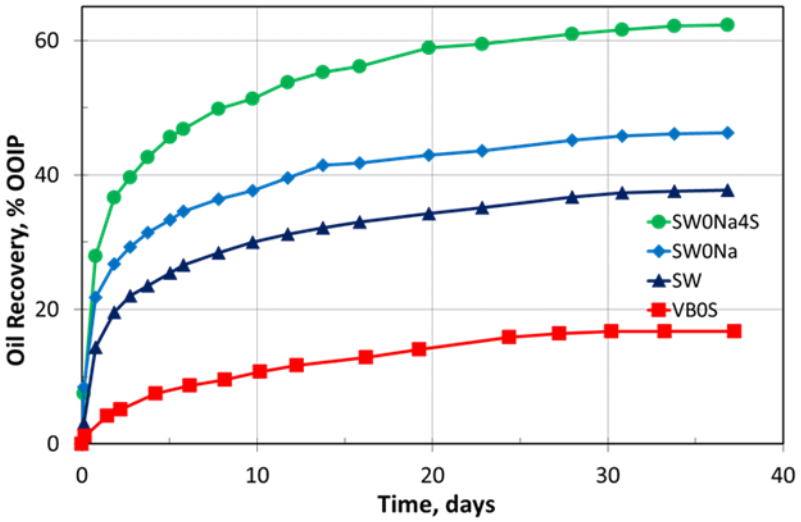

Figure 4.2 SI tests on equally restored chalk cores at 90 ºC. Modified SW as Smart Water imbibing brines (Zhang, 2006)

After experimenting with how SW affects the oil recovery positively in chalk cores repeatedly, studies have been focused on the factors that could affect SW and its wettability modifying capabilities. Factors such as ionic composition, ionic concentrations, and temperature have been studied in this regard to understand their contribution to the wettability-altering effect of SW.

4.2.1 Na^+ Effect

Zhang's (Zhang, 2006) study experiments how Na^+ affects oil recovery. Zhang has done this by removing Na^+ from the injection brine of SW. A core is then spontaneously imbibed at 90 ºC with Na^+ removed SW and around extra 10% of OOIP oil is recovered compare to such by SW (Figure 4.2). This indicates that removing Na^+ from SW enhances the wettability alteration capability of SW at 90 ºC.

4.2.2 SO_4^{-2} Effect

In the same study (Zhang, 2006), Zhang also tests SO_4^{-2} effect. Zhang uses a SW with zero Na^+ and SO_4^{-2} concentration is spiked to four times of the original SW as an imbibing brine. A core is spontaneously imbibed with the brine and it is seen that SW with zero Na^+ and spiked SO_4^{-2} brine recovers an extra 18% of OOIP compare to SW with zero Na^+, giving an ultimate recovery of 62% of OOIP (Figure 4.2). This confirms that SO_4^{-2} is an important ion for wettability alteration and increasing SO_4^{-2} concentration from zero to four times spiked to original SW, improves the wettability alteration capability of SW remarkably at 100 ºC.

Zhang additionally tests the SO_4^{-2} effect separately (Figure 4.3) by experimenting spontaneous imbibition with different brines with different SO_4^{-2} concentrations. In his study (Zhang, 2006), Zhang uses SW as a base brine and prepares 5 SW with changing SO_4^{-2} concentrations. Recovery results confirm that as SO_4^{-2} concentration of SW affects and increasing the SO_4^{-2} concentration enhances the wettability modification capability of SW at 100 ºC.

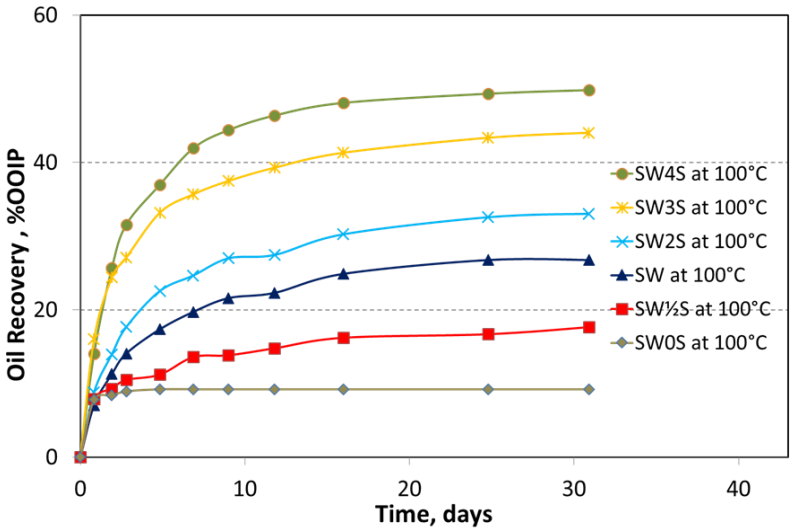

Figure 4.3 SI test results on equally restored chalk cores at 100 C

4.2.3 Ca^{+2} Effect

The Ca^{+2} effect also has been researched by Zhang (Zhang, 2006). In the study, equally restored chalk cores have experimented with SI using five imbibing brines with different Ca^{+2} concentrations at 70 ºC. Imbibing brines are prepared based on SW. SI oil recovery results in Figure 4.4 show that an increase in Ca^{+2} concentration affects the wettability alteration potential of SW significantly and results in better oil displacement hence better oil recovery.

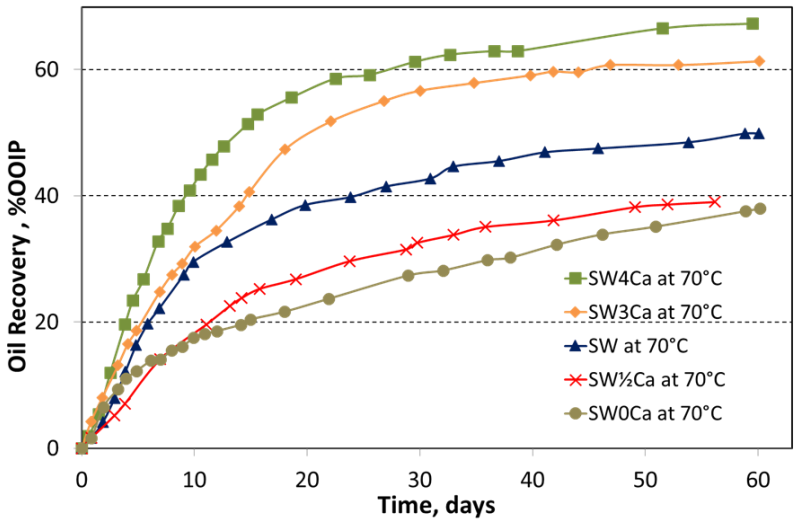

Figure 4.4 SI on equally restored chalk cores at 70 C. SW brines with increasing Ca concentration as imbibing brine.

4.2.4 Mg^{+2} Effect

Zhang states (Zhang et al., 2007b) that another important ion for wettability alteration in carbonates is Mg^{+2}. In the study, equally restored chalk cores are tested with SI with different brines, and oil recovery results were presented in Figure 4.5.

CM-1 core was spontaneously imbibed at 100 ºC with a brine SW0 (no Ca^{+2}, no Mg^{+2}, 1x SO_4^{-2}) and resulted in around 12% of OOIP, and then on day 43, SW amount of Mg^{+2} was added to the SI brine and resulted in extra 20% of OOIP compare to the SW0. This result shows that Mg^{+2} has wettability altering properties in chalk at 100 ºC.

In the same study, Zhang also shows an interesting effect of Mg^{+2}. As shown in Figure 4.5, at 100 ºC, SI shows similar results for CM-2 and CM-4 cores that were being imbibed with brines SW0-0S (no Ca^{+2}, no Mg^{+2}, no SO_4^{-2}) and SW0-4S (no Ca^{+2}, no Mg^{+2} $4xSO_4^{-2}$) respectively and giving around 12% OOIP until the day 53. This shows in the absence of Ca^{+2} and Mg^{+2}, SO_4^{-2} loses its wettability modifying capability at 100 ºC for chalk. Later in the same experiment, on day 53, SW amount of Mg^{+2} was added to both of the imbibing brines to see the combined Mg^{+2}-SO_4^{-2} effect on both of the brines. Adding Mg^{+2} to SW0-0S, resulted in an extra 10% of OOIP while adding Mg^{+2} to SW0-4S brine, resulted in an extra 30% of OOIP. Even though adding Mg^{+2} to the brine enhances wettability alteration for both of the brines, a significant recovery difference is reported with the brine involving $4xSO_4^{-2}$. It is concluded that the SO_4^{-2} effect is very limited if Ca^{+2} and Mg^{+2} are not present in the brine.

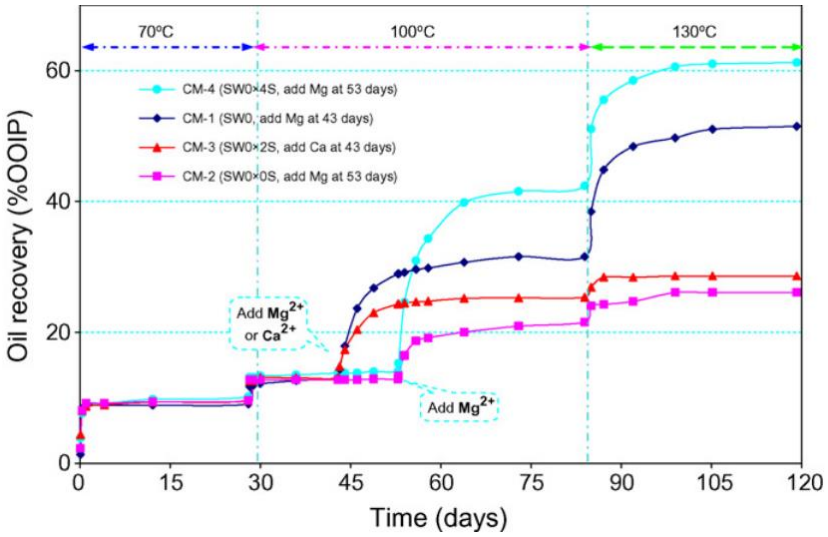

Figure 4.5 SI tests done at 70 ºC, 100 ºC, and 130 ºC. Modified SW without Ca^{+2} and/or Mg^{+2} was used as initial imbibing brine and later on Mg^{+2} and Ca^{+2} were added with the same concentrations in SW

4.2.5 Temperature Effect

Strand et al. (Strand et al., 2008) study and show the effect of temperature on wettability alteration for chalk core by using seawater sequentially with spontaneous imbibition and viscous flooding. As presented in Figure 4.6, seawater at 90 ºC, has a very weak wettability modification capability showed by a slight increase in oil recovery. SI results show an oil recovery increase of 2% of OOIP.

However, at 120 ºC, seawater shows a powerful wettability modification for both spontaneous imbibition and viscous flooding as presented in Figure 4.7. At 120 ºC, core C#6 is spontaneously imbibed with formation water recovering 12% of OOIP and then imbibing brine was changed from FW to SW, giving a total recovery of 30% of OOIP. This extra 18% of OOIP oil recovery confirms that only by switching from formation water to seawater without any changes in the viscous forces, Smart Water EOR effects are present.

Hence, wettability alteration in chalk cores by using seawater exists and is related to the temperature. The wettability modification increases as temperature increases. (Strand et al., 2008)

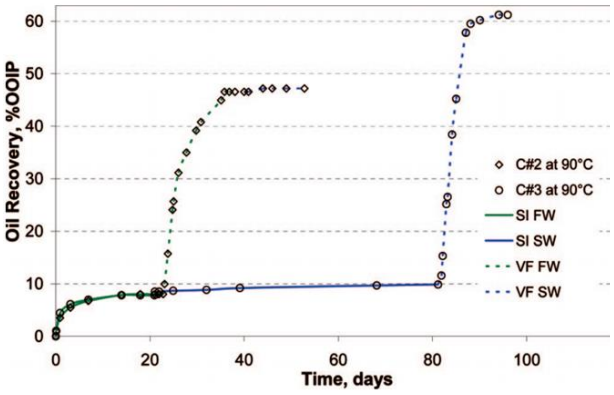

Figure 4.6 Oil recovery at 90 ºC by successive spontaneous imbibition and forced displacement

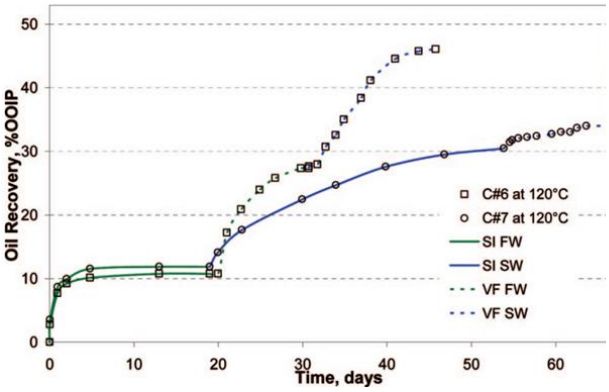

Figure 4.7 Oil recovery at 120 ºC by successive spontaneous imbibition and forced displacement

4.3 Smart Water

An optimized Smart Water composition for chalk has previously been studied. Seawater behaves as a Smart Water at high temperatures. At lower temperatures, the efficiency of seawater could be improved by optimizing ionic composition.

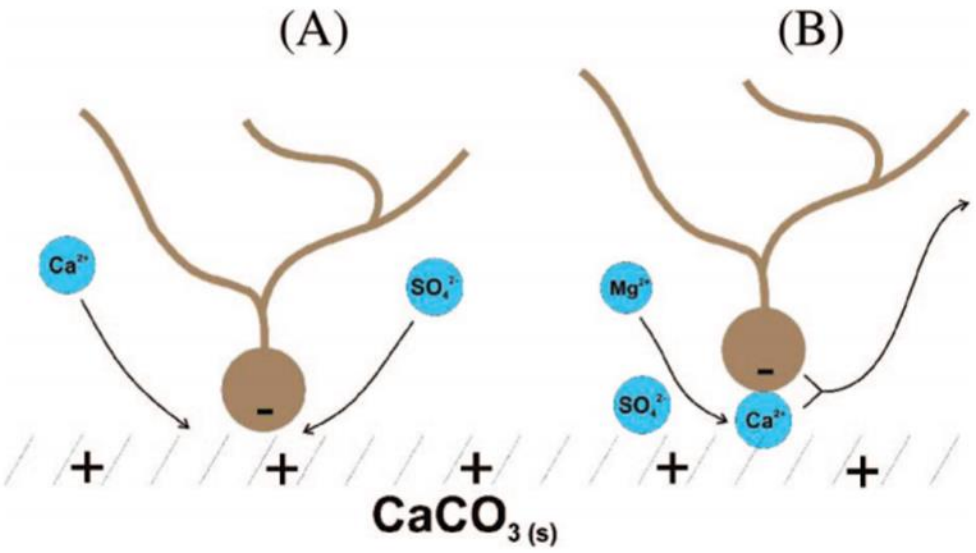

Figure 4.8 Suggested wettability alteration mechanism with seawater

Figure 4.8 illustrates the suggested (Torrijos et al., 2017) wettability alteration mechanism in chalk by seawater (A) when Ca^{+2} and SO_4^{-2} are active and (B) when Mg^{+2} and SO_4^{-2} are active at high temperatures.

Design of Smart Water for carbonates roughly relies on:

- Reduced concentration of NaCl
- An optimum concentration of SO_4^{-2}, $Ca^{+2,}$ and Mg^{+2}
- The optimum concentration should be considered as high enough to provide maximum wettability alteration and low enough not to cause any salt precipitation for the temperature of interest.
- The Smart Water effect of Mg^{+2} should also not be overlooked and should be considered in the availability of Mg^{+2} such as Smart Water designs for dolomite reservoirs.

In the case of having access to pure water, a low concentrated sulfuric acid solution can be prepared to produce an injection brine with the desired SO_4^{-2} concentration. By injecting this brine into $CaCO_3$ reservoirs, the desired Ca^{+2} concentration can be achieved due to $CaCO_3$ dissolution in the near-wellbore of the injection well. Therefore, it is suggested that a Smart Water with selected Ca^{+2} and SO_4^{-2} concentrations can be produced in-situ by injecting H_2SO_4 into the chalk reservoirs.

In the next part, the efficiency of a sulfuric acid-based Smart Water is evaluated for chalk and compared with the efficiency of seawater at 130 ºC that provides an analogy to the Ekofisk field.

5 Experimental Work

5.1 Materials

5.1.1 Oil

A base oil, Res-40, was prepared by diluting Heidrun crude oil with n-heptane in a volume ratio of 60:40. Res-40 oil was treated with silica gel to remove surface-active components from it. After being treated with silica gel, Res-40 was centrifuged and filtered through a 0.5 µm Millipore filter. This treated oil was called Res-40-zero, implying it having very low surface-active components. Res-40 and Res-40-zero mixed regarding Equation 5.1 to obtain Oil-A with the acid number (AN)= 0.53 mgKOH/g and base number (BN)=0.31 mgKOH/g. Oil-A was used throughout the experiment.

$$AN_{Target} = AN_{Res-40} x \frac{V_{Res-40}}{V_{Res-40} + V_{Res-40-zero}} + AN_{Res-40-zero} x \frac{V_{Res-40-zero}}{V_{Res-40} + V_{Res-40-zero}} \quad 5.1$$

Table 5.1 Measured Oil Properties

Oil Name	Density (g/cm^3)	AN (mgKOH/g oil)	BN (mgKOH/g oil)	Viscosity (cP)
Res-40	0.82	1.85	0.67	2.7
Res-40-zero	0.81	0.01	0.03	2.4
Oil-A	0.81	0.53	0.31	2.5

5.1.2 Core Material

All cores that have been used in this research study, obtained from Stevns Klint outcrop chalk in Sjælland, Denmark. Cores were drilled in the same direction and from the same rock block. Cores were then shaven and cut into desired dimensions. The cores used in this research study are presented in Table 5.1. Core #1; Core #2; Core #4; Core #6 were used for the oil recovery test while Core #5 was crushed into chalk powder to be used in the $CaCO_3$-H_2SO_4 batch test.

Table 5.2 Measured Core Properties

Core Name	Length (cm)	Diameter (cm)	Bulk Volume (ml)	Pore Volume (ml)	Porosity (fraction)	k (mD)	Swi (%)	OOIP (ml)
Core #1	7.21	3.79	81.34	38.86	0.4778	4.08	10	34.97
Core #2	7.02	378	78.78	37.87	0.4807	4.00	10	34.08
Core #4	7.22	3.79	81.45	38.61	0.4741	3.61	10	34.75
Core #5	7.10	3.79	80.10	35.32	0.4410	3.77	-	-
Core #6	7.27	3.78	81.58	38.40	0.4707	3.93	10	34.56

5.1.3 Brines

Brines used in this research study were prepared synthetically in the laboratory regarding the compositions in Table 5.3 Brine Compositions and Properties. To avoid possible precipitations during brine preparation, salts involving CO_3^{-2}, Cl^-, and SO_4^{-2} dissolved separately in de-ionized water. After visual assurance of having no salt precipitation in the mixtures, mixtures combined to obtain individual brines. Brines then were filtered through 0.22 µm Millipore filters.

5.1.3.1 Valhall brine

Valhall brine, the formation water characterized from the Valhall field located in the southern North Sea, was chosen in this research study to be studied with as formation water. Moreover, to see the possible effects of SO_4^{-2} on wettability and oil recovery, Valhall brine was prepared without any SO_4^{-2} in it and this brine was called Valhall brine zero sulfates (VB0S). VB0S was used as imbibing fluid for spontaneous imbibition tests for Core #1 and Core #6 besides being formation water as in initial water saturation for all cores studied.

5.1.3.2 Sea Water

Sea Water was prepared to be used as the imbibing fluid for the spontaneous imbibition test for Core #2 and Core #6.

5.1.3.3 CaSO_4 Solution-*Smart Water*

CaSO_4 solution was prepared regarding $CaCO_3$-H_2SO_4 batch test results to be used as the imbibing fluid for the spontaneous imbibition test for Core #4 and Core #1.

Table 5.3 Brine Compositions and Properties

Ions	FW (mM)	SW (mM)	Smart Water (mM)
HCO_3^-	9	2	0
Cl^-	1066	525	0
SO_4^{-2}	0	24	10
Mg^{+2}	8	45	0
Ca^{+2}	29	13	10
Na^+	997	450	0
K^+	5	10	0
Density, g/cm^3 at 20 ºC	1.041	1.022	0.999
TDS, g/l	62.83	33.39	1.72
Ca^{+2}/SO_4^{-2}	N/A	0.540	1

5.2 Methodology

5.2.1 Core Cleaning

Cores were cleaned with a procedure characterized by Puntervold (Puntervold et al.2007). Cores were flooded with 5 PV of de-ionized water with a flow rate of 0.1 ml/min at room temperature. Effluent samples were collected to test both qualitatively to see SO_4^{-2} presence in the effluent samples if there were any and quantitatively to confirm cleaning of easily removable salts from the rock surface. Qualitative tests were performed by adding $BaCl_2$ to effluent samples to see any probable $BaSO_4$ precipitation. Quantitative tests performed by Ion Chromatography. Both quantitative and qualitative SO_4^{-2} test results are presented in the Appendix.

5.2.2 Porosity Measurement

Cores dried at 90 ºC to a constant weight. Dried cores weighted to measure $w_{dry.}$ Cores then were saturated in a vacuum cell with de-ionized water. Porosity, φ, in fraction was calculated by using w_{dry} and $w_{saturated}$, in g, ρ_{DI}, in g/cm^3 and V_{bulk} in cm^3 of the core as shown in Equation 5.2

$$\varphi = \frac{\frac{w_{saturated}}{\rho_{DI}}}{V_{bulk}} \qquad 5.2$$

Where,

φ, the porosity of the core, fraction

$w_{saturated}$, the weight of the saturated core, g

ρ_{DI}, density of de-ionized water at 20 ºC, g/cm^3

V_{bulk}, the bulk volume of the core, cm^3

5.2.3 Permeability Measurement

Permeability measurements were performed in a flooding setup at room temperature with 8 bar of backpressure to ensure control over pressure difference, ΔP, between inlet and outlet. Each core flooded with de-ionized water with flow rates of 0.1 ml/min, 0.3 ml/min, and 0.5 ml/min. Pressure differences were recorded for corresponding flowrates and permeability, k in mD was calculated according to Equation 5.3

$$k = \frac{Q\ \mu\ L}{\Delta P\ A} \qquad 5.3$$

where:

k, the rock permeability, D

Q, the flowrate, ml/s

μ, viscosity of flooding fluid, cP,

L, the length of the core, cm

A, the cross-sectional flow area, cm^2

ΔP, the pressure difference between inlet and outlet, atm

After the permeability measurement, the core dried at 90 ºC to a constant weight.

5.2.4 Establishing Initial Water Saturation

Knowing the dry weight of the core, target weight of the core with water saturation, S_w=10% were calculated as in Equation 5.4. The cleaned and dried core was fully saturated in a vacuum cell with 10 times diluted Valhall brine (d10VB0S) (Springer et al. 2003). A fully saturated core was placed in a desiccator with silica gel at the bottom to absorb water from the core. Core weight was measured frequently until it reached the target weight. Once the core reached the target weight, the initial water saturation of 10% with VB0S was ensured to be established. After establishing initial water saturation, the core was secured in a sealed container to rest for 3 days to let the introduced brine diffuse all over the core.

$$w_{target} = w_{dry} + (0.1 x PV x \rho_{VB0S}) \qquad 5.4$$

where:

w_{target}, the weight of the core with S_w=10%, g

w_{dry}, the weight of the dry core, g

PV, pore volume, ml

ρ_{VB0S}, density of the VB0S Brine, 1.0224 g/cm^3

5.2.5 Establishing Oil Saturation

Core with S_w=10% was placed in a Hassler core holder in a heating set-up. The air in the pore space of the core was vacuumed before oil injection to provide an air-free oil saturation. After the vacuum was completed, 1 PV of Oil A was injected from both sides of the core with an injection rate of 0.165 ml/min. 2 PV of Oil A then was injected in direction of from right to left. Later 2 PV of Oil A was injected in direction of from left to right. After oil injection and flooding, the saturated core was weighted to confirm aimed oil saturation, S_o=90%.

5.2.6 Aging Phase

Core with initial water and oil saturations wrapped in PTFE film tape to protect their constituents. Cores then were left aging at 130 ºC for 14 days with a support cell filled with Oil A and pressurized to 10 bars to avoid evaporation or volatilization of the fluids.

5.2.7 Spontaneous Imbibition Test

Aged core placed in a steel imbibition cell filled with imbibing fluid connected to a piston cell filled with imbibing fluid and pressurized at 10 bar to provide pressure support. 10 bar of pressure support was important to keep fluids in the imbibition cell and core in the liquid phase at 130 ºC of imbibing temperature. Produced oil was collected and oil volume was recorded to calculate Original Oil in Place, %OOIP.

5.2.8 $CaCO_3$-H_2SO_4 Batch Test

The batch test was performed to determine what maximum Ca^{+2} and SO_4^{-2} concentrations are possible without any precipitation in the pore water- H_2SO_4 - $CaCO_3$ system. The test was performed at 110 ºC, 120 ºC, and 130 ºC and by adding 1 g of powdered rock into differently concentrated, 6mM; 8mM; 10mM; 12mM, H_2SO_4 solutions. Later samples were placed in a rotator setup in a heating system and let chemically equilibrate. After rock-acid interaction stabilized, samples were centrifuged and liquid phase filtered through a 0.2 µm Pall Acrodisc filter. Filtered samples were analyzed in ion chromatography to determine ion concentrations, higher focus was done on Ca^{+2} and SO_4^{-2} in the samples. After determination maximum, possible concentrations were used to prepare the $CaSO_4$-Smart Water Brine.

6 Results

6.1 Core Cleaning

The results confirm that the ion concentration in effluents from Core #1 is rather low (Figure 6.1), reaching a minimum concentration of ions after about 3.5 PV injection of DI water. The concentration of Mg^{+2} and K^{+} is low, while the concentration of Ca^{+2} and SO_4^{-2} steadily declines and reaches a minimum after about 3 PV injected. SO_4^{-2} is retained more strongly than Ca^{+2}.

With a low Mg^{+2} concentration, the salts present in the core material most likely have an origin of Gypsum/Anhydrite and not seawater.

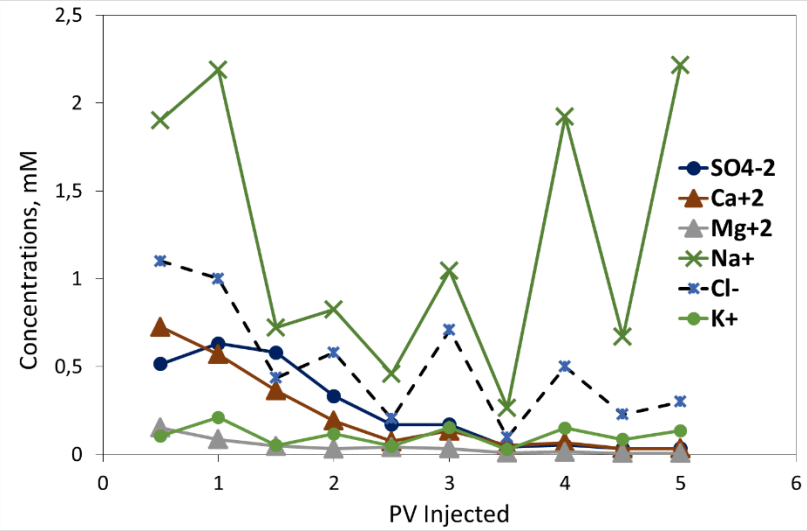

Figure 6.1 Core cleaning results for all ions for Core #1

The results from all the core cleaning experiments are summarized in Figure 6.2-Figure 6.7, confirming reproducible trends from Core #1.

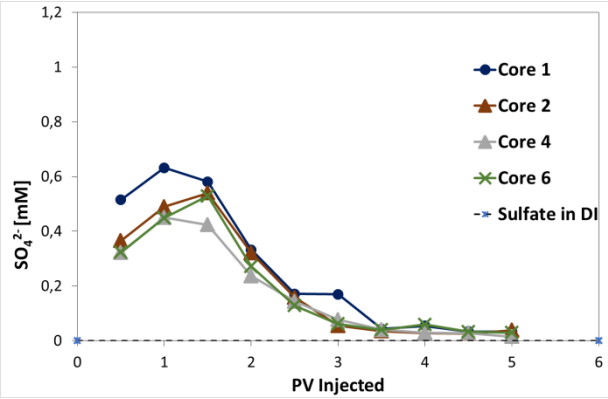

Figure 6.2 Ion chromatography results for core cleaning for [SO_4^{-2}]

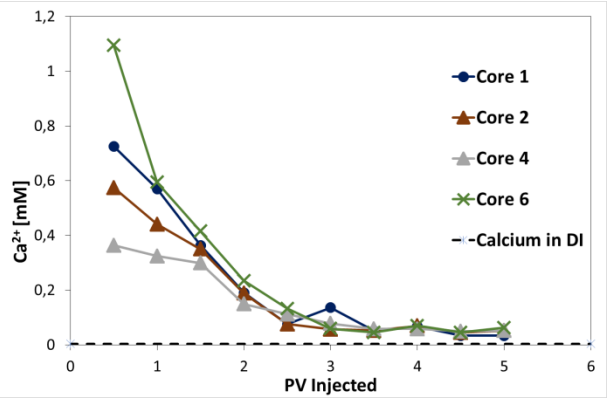

Figure 6.3 Ion chromatography results for core cleaning for [Ca^{+2}]

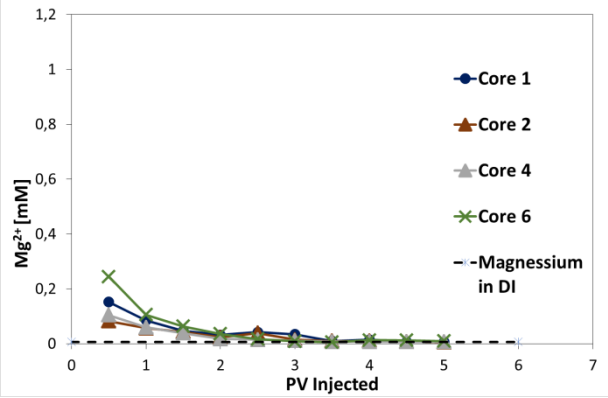

Figure 6.4 Ion chromatography results for core cleaning for [Mg^{+2}]

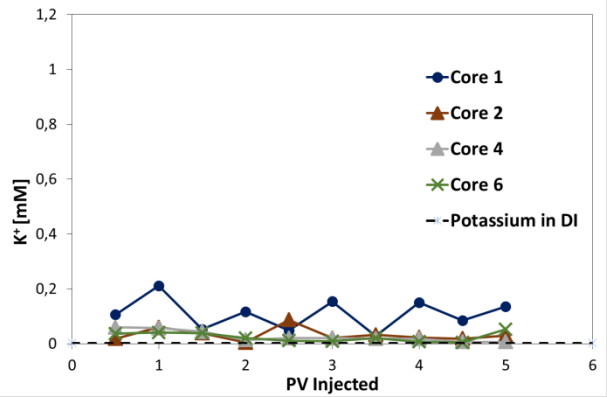

Figure 6.5 Ion chromatography results for core cleaning for [K^+]

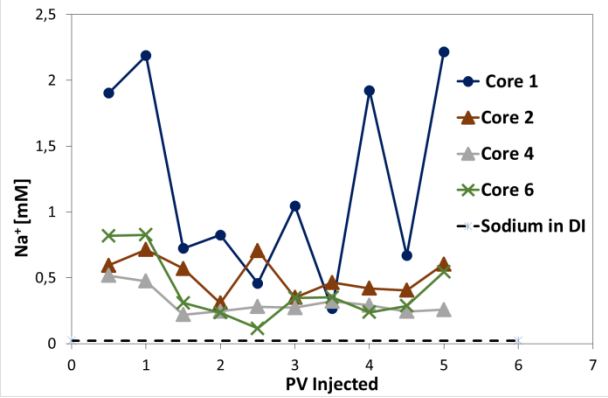

Figure 6.6 Ion chromatography results for core cleaning for [Na^+]

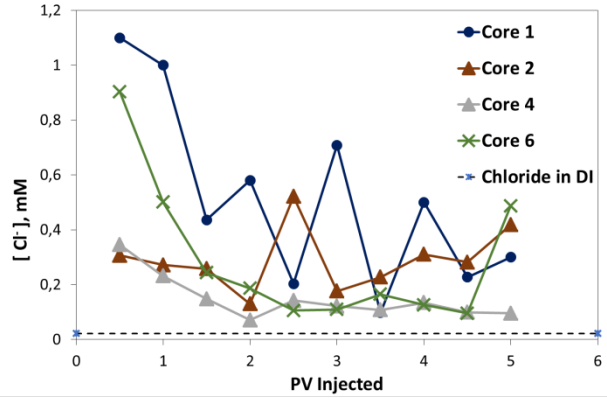

Figure 6.7 Ion chromatography results for core cleaning for [Cl^-]

6.2 Porosity and Permeability Measurement

6.2.1 Porosity Measurement

Rock porosities of the cores are measured according to Equation 6.1 and results are presented in Table 6.1

$$\varphi = \frac{\frac{w_{saturated}}{\rho_{DI}}}{V_{bulk}} \qquad 6.1$$

Where,

φ the porosity of the core, fraction

$w_{saturated}$ the weight of the saturated core, g

ρ_{DI} density of de-ionized water at 20 ºC, g/cm^3

V_{bulk} the bulk volume of the core, cm^3

Table 6.1 Porosity Measurement Results

Core Name	Porosity (fraction)
Core #1	0.4778
Core #2	0.4807
Core #4	0.4741
Core #5	0.4410
Core #6	0.4707

6.2.2 Permeability Measurement

Rock permeabilities in this study were measured with a flooding setup. Cores were flooded with formation water with flow rates of 0.1 ml/min, 0.3 ml/min, and 0.5 ml/min. Corresponding pressure differences were recorded to calculate permeabilities according to Equation 5.3. Recorded pressure differences for corresponding flow rates and permeabilities are presented in Table 6.2.

$$k = \frac{Q\ \mu\ L}{\Delta P\ A} \qquad 5.3$$

Where:

k the rock permeability, D

Q the flow rate, ml/s

μ viscosity of flooding fluid, cP

L the length of the core, cm

A the cross-sectional flow area, cm^2

ΔP the pressure difference between inlet and outlet, atm

Table 6.2 Permeability Measurement Results

	Q, ml/min	ΔP, mbars	k, mD	Average k, mD
Core #1	0.1 0.3 0.5	235 722 1200	4.14 4.05 4.06	4.08
Core #2	0.1 0.3 0.5	239 719 1182	3.99 3.98 4.04	4.00
Core #4	0.1 0.3 0.5	267 813 1349	3.63 3.59 3.60	3.61
Core #5	0.1 0.3 0.5	258 773 1290	3.77 3.78 3.77	3.77
Core #6	0.1 0.3 0.5	251 757 1263	3.94 3.92 3.92	3.93

Table 6.3 summarizes the porosities and permeabilities of the cores. The porosity values of the cores range between 0.4410 and 0.4807 while permeabilities of the cores range between

3.61-4.08 mD. Results present that all the cores have similar porosity and permeabilities that can be considered high porosity and low permeability.

Table 6.3 Porosity and Permeability Summarized Results

Core Name	Porosity (fraction)	k (mD)
Core #1	0.4778	4.08
Core #2	0.4807	4.00
Core #4	0.4741	3.61
Core #5	0.4410	3.77
Core #6	0.4707	3.93

6.3 $CaCO_3$-H_2SO_4 Batch Test

A batch test was performed to determine the maximum possible SO_4^{-2} and Ca^{+2} concentration without causing precipitation. Maximum possible concentrations were used to prepare the $CaSO_4$-Smart Water brine. The batch test was performed at three different temperatures, 110 ºC, 120 ºC, and 130 ºC.

Acidification reaction Equation 6.2 states that as H_2SO_4 concentration increases, equilibrium moves towards the right, and yields more products. After a critical value of sulfuric acid concentration, Equation 6.3 takes place in the right direction and $CaSO_4$ starts to precipitate.

$$CaCO_{3\,(s)} + H_2SO_{4\,(aq)} \leftrightharpoons Ca^{2+} + CO_{3\,(aq)}^{2-} + 2H_{(aq)}^{+} + SO_{4\,(aq)}^{2-} \qquad 6.2$$

$$Ca_{(aq)}^{2+} + CO_{3\,(aq)}^{2-} + 2H_{(aq)}^{+} + SO_{4\,(aq)}^{2-} + HEAT \leftrightharpoons CaSO_{4\,(s)} + CO_{2\,(g)} + H_2O_{(l)} \qquad 6.3$$

Due to the endothermic nature of the reaction Equation 6.3, as temperature increases, equilibrium moves towards the right and yields more products meaning Equation 6.3 produces more reaction product in other words, causes $CaSO_4$ precipitation.

Results of the batch test are summarized in Table 6.4. The bold figures indicate the conditions that $CaSO_4$ precipitation happen.

Table 6.4 Ion Chromatography Analysis of the equilibrated $CaCO_3$-H_2SO_4 solutions

	T=110 ºC		T=120 ºC		T=130 ºC	
$H_2SO_4^{-2}$ [mM]	SO_4^{-2} [mM]	Ca^{2+} [mM]	SO_4^{-2} [mM]	Ca^{2+} [mM]	SO_4^{-2} [mM]	Ca^{2+} [mM]
5.72	5.29	4.68	5.13	3.31	4.54	3.36
7.70	7.27	6.32	6.84	4.84	8.67	9.21
9.23	8.85	6.86	8.59	7.08	10.25	12.92
13.5	12.08	9.94	**7.17**	**5.83**	**6.98**	**7.68**

Figure 6.8 shows how non-associated SO_4^{-2} concentration in the effluent samples changes as SO_4^{-2} concentration in bulk acid increases. As the figure illustrates, SO_4^{-2} concentration in the effluent samples increases as SO_4^{-2} concentration in bulk acid increases expectedly until a critical value of SO_4^{-2} concentration in bulk acid. After this critical value, even though SO_4^{-2} concentration in bulk acid continues to increase, SO_4^{-2} concentration in the effluent samples begins to decrease. This decrease indicates precipitation of SO_4^{-2} salts after the critical bulk acid concentration regarding dissolution reaction Equation 6.2.

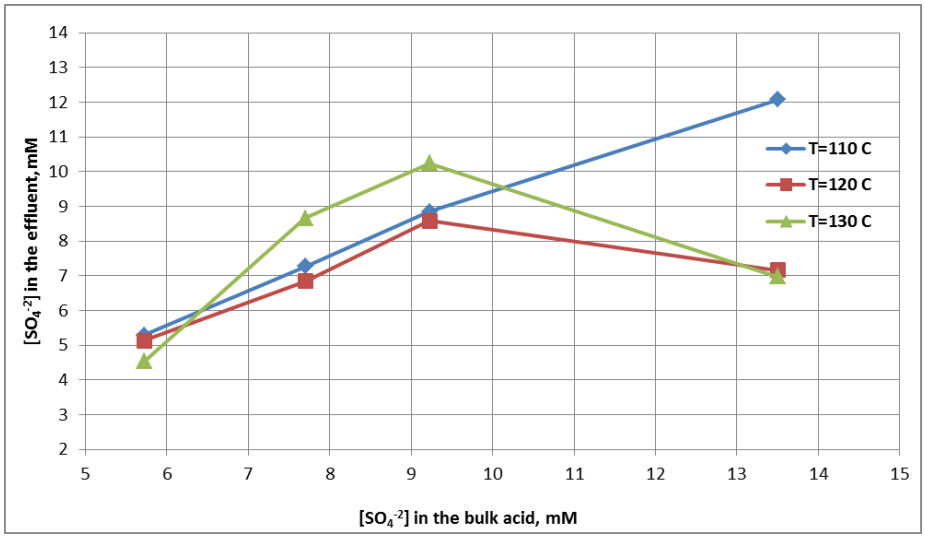

Figure 6.8 Free SO_4^{-2} concentration in $CaCO_3$-H_2SO_4 solutions.

Similarly, Figure 6.9 illuminates how Ca^{+2} concentration in the effluent samples changes as SO_4^{-2} concentration in bulk acid increases. The figure clarifies how Ca^{+2} concentration in the effluent samples builds up as SO_4^{-2} concentration in bulk acid increases till it reaches a critical value of SO_4^{-2} concentration in bulk acid. After the critical value, Ca^{+2} concentration in the effluent samples starts to decrease rapidly. This rapid decrease shows precipitation of Ca^{+2} salts after the critical bulk acid concentration.

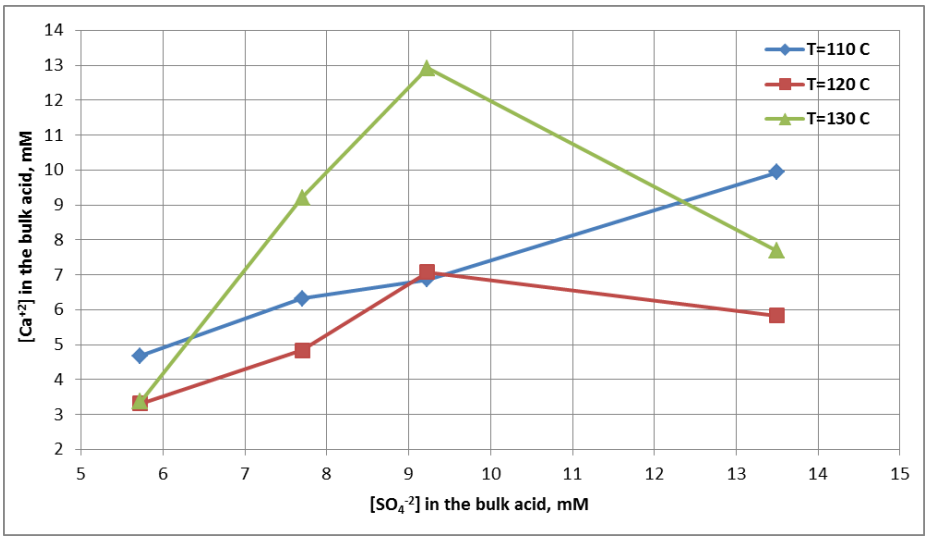

Figure 6.9 Free Ca^{+2} concentration in $CaCO_3$-H_2SO_4 solutions.

The precipitation of both SO_4^{-2} and Ca^{+2} salts can affect the porous system negatively not only due to damaging porous flow by decreasing porosity and permeability but also due to decreasing concentrations of potential determining ions like SO_4^{-2} and Ca^{+2} which are critical for wettability alteration by Smart Water processes in carbonates. Hence, determining maximum SO_4^{-2} and Ca^{+2} concentration that does not cause precipitation is important for Smartt Water design.

The batch test results confirm that a maximum of 10 mM SO_4^{-2} could be present in the solution without significant precipitation. Therefore a sulfuric acid based Smart Water is designed for chalk at 130 °C based on injection of 10 mM sulfuric acid solution into chalk.

6.4 The Efficiency of a Sulfuric Acid Based Smart Water

The efficiency of the sulfuric acid based smart water has been evaluated by spontaneous imbibition experiments at 130 ºC.

4 cores have been restored with initial water saturation, S_{wi} of 10%, and exposed to the same amount of crude oil with AN = 0.53 mgKOH/g and BN=0.31 mgKOH/g, to achieve the same initial core wettability.

The cores have then been spontaneously imbibed with different brines. FW was used to evaluate the initial core wettability after core restoration.

SW was used as an imbibing brine to evaluate the efficiency of SW for wettability alteration.

H_2SO_4 based $CaSO_4$ solution was used as an imbibing brine to evaluate if it could be used as a Smart Water injection brine for chalk at 130 ºC.

6.5 Spontaneous Imbibition

6.5.1 Initial core wettability

Spontaneous imbibition of the restored Core #1 and Core #6 was performed using FW as imbibing brine. The imbibing brine has the same composition as the one initially presented into the restored cores to avoid any chemically induced wettability alteration during the experiments.

The results from the spontaneous imbibition of Core #1 and Core #6 are shown in Figure 6.9 and Figure 6.10 respectively. The SI results confirm an ultimate recovery of 31 %OOIP for Core #1 reached after 11 days, and the ultimate recovery of 30 %OOIP for Core #6 reached after 6 days.

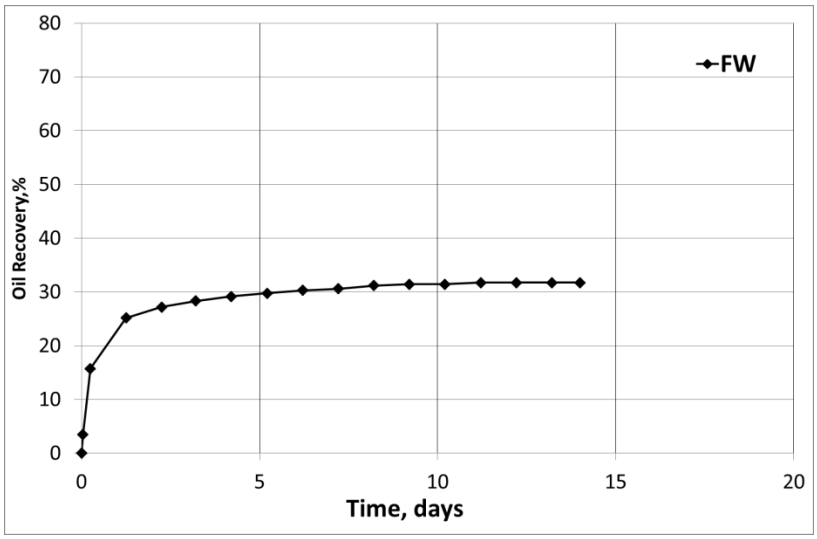

Figure 6.9 Oil Recovery with Spontaneous Imbibition by FW-Core #1

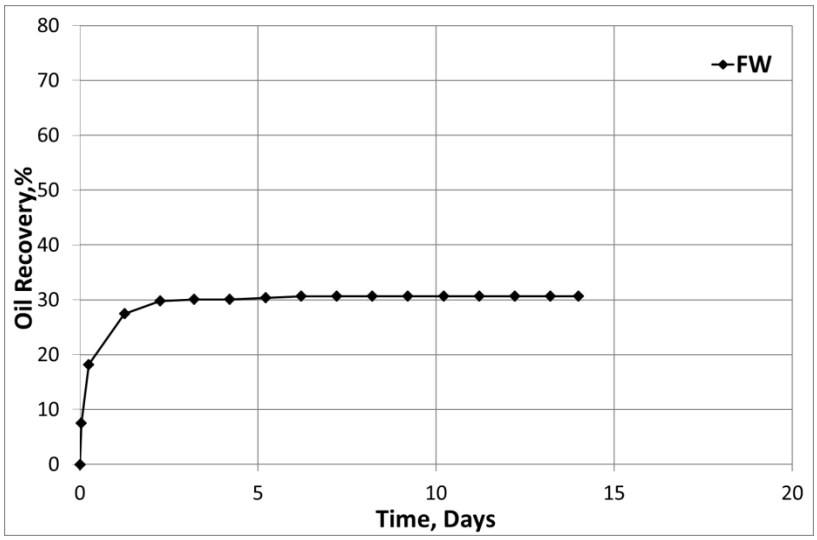

Figure 6.10 Oil Recovery with Spontaneous Imbibition by FW-Core #6

The SI experiments with FW confirm that recovery trends between the individual core experiments were reproducible. Slightly water-wet wettability was expected in all restored cores that had been used in this work.

6.5.2 Smart Water EOR Effects in Tertiary Mode

After spontaneous imbibition by FW in Core #6, the imbibing brine was changed to SW. The oil recovery result is presented in Figure 6.11.

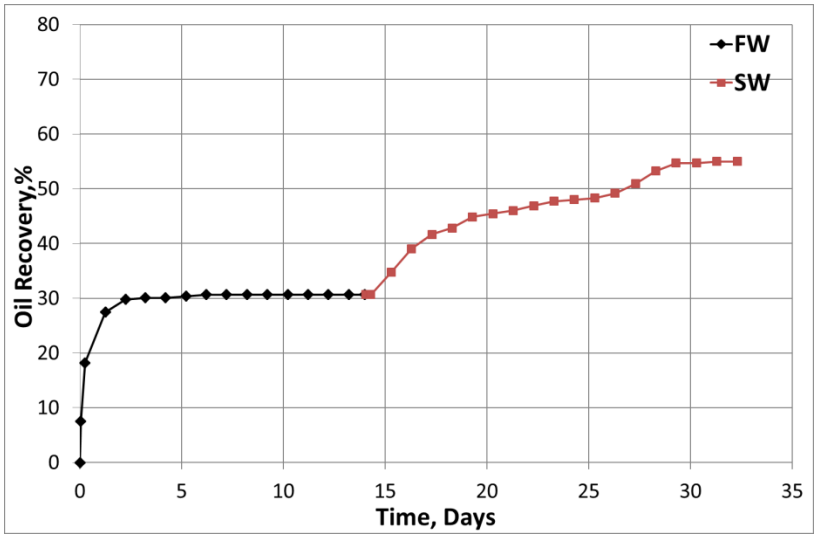

Figure 6.11 Oil Recovery with Spontaneous Imbibition by FW/SW-Core #6

Figure 6.11 illustrates that after changing imbibing brine from FW to SW, extra oil was produced. Ultimate recovery of 55% OOIP is reached in 14 days. This additional oil recovery indicates that SW can change the initial wettability conditions towards more water-wet.

The efficiency of $CaSO_4$ brine as a Smart Water has been tested in tertiary mode by changing the imbibing brine of Core #1 from FW to 10 mM $CaSO_4$ brine.

SI results for Core #1 in tertiary mode are shown in Figure 6.12.

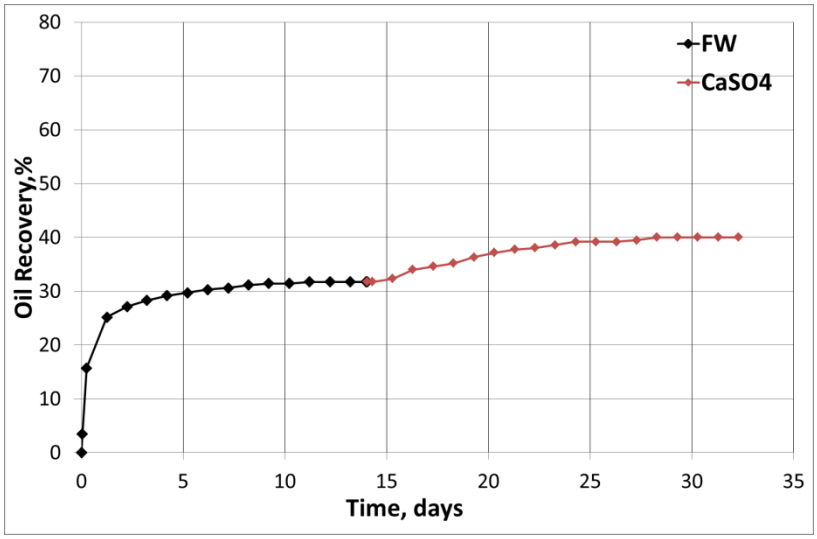

Figure 6.12 Oil recovery with spontaneous imbibition by FW/$CaSO_4$-Core #1

Figure 6.12 shows that a slight increase in oil recovery is observed after changing imbibing brine from FW to $CaSO_4$ brine. An ultimate oil recovery of 40% OOIP is reached after 15 days. This slight increase in oil recovery indicates that $CaSO_4$ brine has a weak wettability alteration capability. Comparing Figure 6.11 to Figure 6.12 reveals the efficiency differences between SW and $CaSO_4$ brine when used following FW. Hence the comparison suggests that SW is significantly more efficient than $CaSO_4$ brine.

6.5.3 Smart Water EOR Effects in Secondary Mode

The restored Core #2 was spontaneously imbibed by SW in secondary mode. Oil recovery results are presented in Figure 6.13.

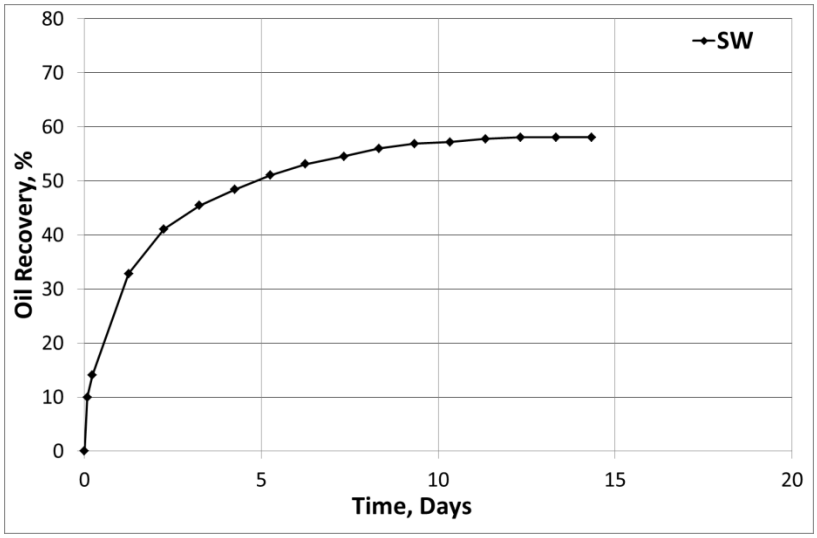

Figure 6.13 Oil recovery with spontaneous imbibition by SW-Core #2

Spontaneous imbibition of Core #2 by SW resulted in an ultimate oil recovery of 58% of OOIP after 13 days, confirming that SW is extremely efficient as a Smart Water in chalk at 130 ºC.

An additional experiment using the $CaSO_4$ brine after SW in tertiary mode was planned but the experiment failed. The restored Core #4 was spontaneously imbibed with $CaSO_4$ brine in secondary mode. The results are presented in Figure 6.14

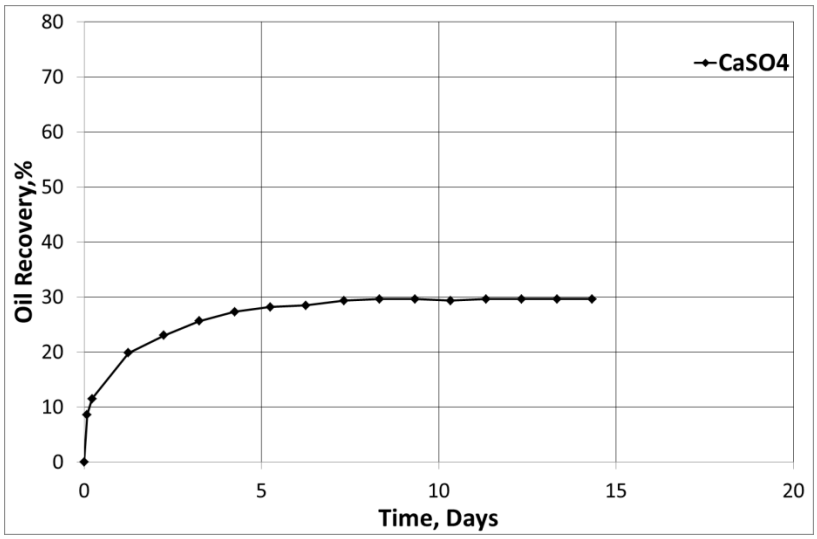

Figure 6.14 Oil recovery with spontaneous imbibition by $CaSO_4$

The ultimate recovery in this experiment gave a result of 30% OOIP after 8 days, close to the results achieved with FW in Core #1 and Core #6, confirming that $CaSO_4$ brine did not behave as a Smart Water in secondary mode at 130°C.

SW was then introduced as Smart Water in tertiary mode. A rapid and significant increase in recovery was observed, reaching an ultimate recovery of 54%OOIP after 8 days, validating that SW acts as Smart Water in chalk at 130°C, Figure 6.15.

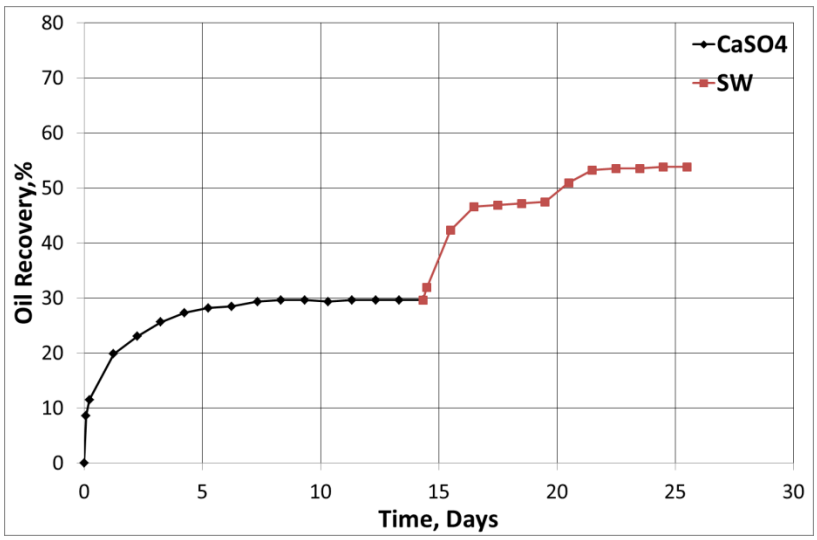

Figure 6.15 Oil recovery with spontaneous imbibition by $CaSO_4$/SW

6.5.4 Wettability Measurement

To quantify the water wetness of the cores used, spontaneous imbibition test results on the same SK Chalk were used (Andreassen et al., 2019). The test was performed on a pre-cleaned SK Chalk core with 10% S_{wi}. The core was saturated with heptane then spontaneously imbibed by FW at 23 ºC. The test results are presented in Figure 6.16, showing an ultimate recovery of 75% of OOIP.

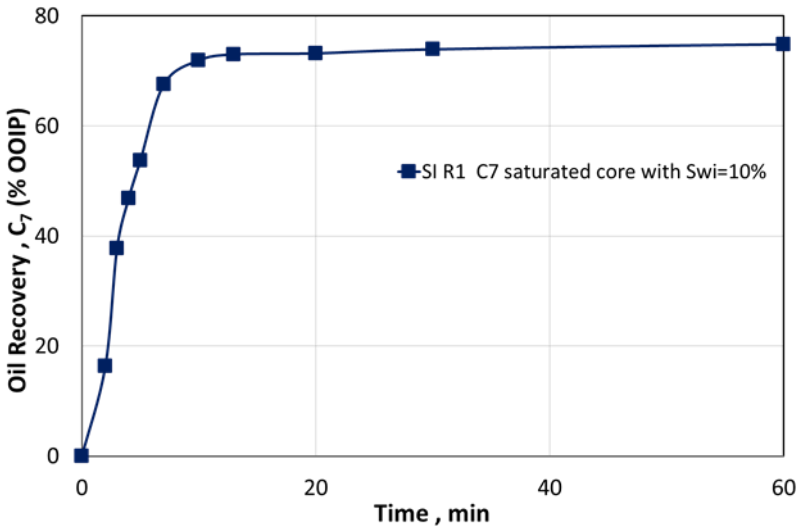

Figure 6.16 SI test results performed in a strongly water-wet SK Chalk core

The core has a strongly water-wet behavior giving an ultimate recovery of 75% of OOIP that was reported reaching in the first 30 minutes. The results confirm strong capillary forces available.

Modified Amott Indices for Core #1 SI by FW can be solved as in Equation6.4

$$I^*_{W-SI-Core\#1} = \frac{31.7}{75} = 0.42 \qquad 6.4$$

Modified Amott Indices for the other cores similarly calculated as above and presented in Table 6.5.

Table 6.5 Oil Recovery by Spontaneous Imbibition on Secondary and Tertiary Mode at 130 ºC

	Secondary Mode		Tertiary Mode	
	Imbibing Fluid	I^*_{W-SI}	Imbibing Fluid	I^*_{W-SI}
Core #1	FW	0.42	$CaSO_4$	0.54
Core #6	FW	0.41	SW	0.73
Core #2	SW	0.78	$CaSO_4$	*Failed*
Core #4	$CaSO_4$	0.39	SW	0.72

Table 6.5 shows the water wetness of the cores in terms of Modified Amott Indices. Initial water wetness of the cores is and reproduced around 0.4. The results confirm that seawater modifies wettability towards more water-wet states in both secondary and tertiary modes. Also, although $CaSO_4$ brine can change wettability towards water wet, it does not show a strong modifier effect.

7 Discussions

All SK outcrop cores were pre-cleaned before the experiments to avoid ion pollutions in the outcrop material affecting core restoration.

The results confirm that quite similar porosity and permeability properties exist in all cores used.

Core restorations were performed with Swi of 10% and by exposing the cores to equal amounts of crude oil, Oil A, with AN of 0.53 mgKOH/g and BN of 0.31 mgKOH/g. The SI experiments with FW confirmed reproducible wettability results.

SW behaves as a Smart Water at high temperatures in chalk. Ca^{+2} and SO_4^{-2} ions are the main ions contributing to the wettability alteration process.

A Smart Water EOR brine, involving Ca^{+2} and SO_4^{-2} ions, could easily be designed by using low concentrations of sulfuric acid in freshwater and using it as an injection brine for the chalk. Such a brine was tested and compared to SW as an injection brine. It is confirmed by the batch test that the $CaSO_4$ brine can have a maximum of 10 mM concentration of SO_4^{-2} in the solution at 130 °C.

The results in this work also validate that SW is a Smart Water in Chalk at 130°C and very efficiently changes the core wettability towards more water-wet conditions.

The designed $CaSO_4$ brine did not behave as a Smart Water, neither in secondary nor in tertiary mode after FW. The reason for this is not clearly shown with these results. However considering Ca^{+2} and SO_4^{-2} ions have strong impacts on wettability modification capacity, having a lower Ca^{+2} (10mM) and SO_4^{-2} (10mM) concentrations than SW ($[Ca^{+2}]$=13 mM and $[SO_4^{-2}]$=24 mM) is an important factor that might be responsible for the low wettability modification performance of the designed $CaSO_4$ brine.

Knowing that SW has more SO_4^{-2} than $CaSO_4$ brine and performing well without causing significant precipitation, to be able to increase SO_4^{-2} concentration of $CaSO_4$ brine with no precipitation, other ions present in SW should be researched and considered to be added to $CaSO_4$ brine.

If increasing SO_4^{-2} concentration in a $CaSO_4$ brine is targeted, Mg^{+2} ion likely is needed to be added to the brine composition. Mg^{+2} ion is most likely to stabilize the ionic environment in the brine and avoid $CaSO_4$ precipitation by complexing SO_4^{-2} with Mg^{+2}, Mg^{+2}:SO_4^{-2}.

Mg^{+2} concentration in SW is 45 mM, but could probably be significantly reduced, i.e. 24 mM which is equal to the SO_4^{-2} concentration in SW. The optimal Mg^{+2} concentration in a brine involving Mg^{+2}, Ca^{+2}, and SO_4^{-2} needs to be experimentally investigated in further studies.

8 Conclusion

The main conclusions observed from this study are as follows.

Table 8.1 Oil Recovery by Spontaneous Imbibition on Secondary and Tertiary Mode at 130 ºC

	Secondary Mode		Tertiary Mode	
	Imbibing Fluid	%OOIP	Imbibing Fluid	%OOIP
Core #1	FW	31.7	$CaSO_4$	40.1
Core #6	FW	30.7	SW	55.0
Core #2	SW	58.1	$CaSO_4$	*Terminated*
Core #4	$CaSO_4$	29.6	SW	53.8

- The Smart Water concentration was decided after the $CaCO_3$-H_2SO_4 batch test to contain maximum Ca^{+2} and SO_4^{-2} without causing any precipitation. Therefore the study suggested a 10 mM $CaSO_4$ solution as a Smart Water that can alter wettability in chalk carbonate at 130 ºC.
- The Smart Water was tested as the spontaneous imbibition fluid to see any possible wettability altering effects. For Core #1, Smart Water was used in tertiary mode after formation water and resulted in extra oil recovery of 8.4% of OOIP. This extra oil recovery indicates that the wettability-altering capability of the Smart Water is not powerful but exists.
- Seawater also was tested as a spontaneous imbibition fluid to observe any possible wettability modifying effects. For Core #6, seawater was used in tertiary mode after formation water, and extra oil recovery of 24.3% of OOIP was reported. This extra oil recovery confirmed that seawater can alter wettability in favor of oil displacement.
- Smart Water was used as a spontaneous imbibition fluid in the secondary mode as well. The experiment resulted in 29.6% of OOIP oil recovery.
- Seawater also was used as a spontaneous imbibition fluid in the secondary mode and the experiment resulted in 58.1% of OOIP oil recovery.
- Seawater was used as an imbibing fluid in tertiary mode after Smart Water to see if seawater can alter wettability in a Smart Water imbibed core. Core #4 was spontaneously imbibed with Smart Water and resulted in 29.6% OOIP oil

recovery. Then imbibing fluid was changed to seawater and 53.8% of OOIP oil was recovered in total. This extra 24.2% of OOIP oil recovery indicates that seawater is a wettability modifier even after Smart Water.

Appendixes

Spontaneous Imbibition Data

Table 0.1 Spontaneous Imbibition Data for Core #1

Time, Days	Oil Volume, mL	Oil Recovery, %
0.00	0.0	0.00
0.04	1.2	3.43
0.25	5.5	15.73
1.25	8.8	25.16
2.25	9.5	27.16
3.21	9.9	28.31
4.21	10.2	29.17
5.21	10.4	29.74
6.21	10.6	30.31
7.21	10.7	30.59
8.21	10.9	31.17
9.21	11.0	31.45
10.21	11.0	31.45
11.21	11.1	31.74
12.21	11.1	31.74
13.21	11.1	31.74
14.00	11.1	31.74
14.04	11.1	31.74
14.29	11.1	31.74
15.29	11.3	32.31
16.29	11.9	34.03
17.29	12.1	34.60
18.29	12.3	35.17
19.29	12.7	36.31
20.29	13.0	37.17
21.29	13.2	37.74
22.29	13.3	38.03

23.29	13.5	38.60
24.29	13.7	39.17
25.29	13.7	39.17
26.29	13.7	39.17
27.29	13.8	39.46
28.29	14.0	40.03
29.29	14.0	40.03
30.29	14.0	40.03
31.29	14.0	40.03
32.29	14.0	40.03
Time, Days	**Oil Volume, mL**	**Oil Recovery, %**

Table 0.2 Spontaneous Imbibition Data for Core #2

Time, Days	**Oil Volume, mL**	**Oil Recovery, %**
0.00	0.0	0.00
0.08	3.4	9.98
0.23	4.8	14.08
1.25	11.2	32.86
2.25	14.0	41.08
3.25	15.5	45.48
4.25	16.5	48.41
5.25	17.4	51.05
6.25	18.1	53.11
7.33	18.6	54.57
8.33	19.1	56.04
9.33	19.4	56.92
10.33	19.5	57.21
11.33	19.7	57.80
12.33	19.8	58.09
13.33	19.8	58.09
14.33	19.8	58.09
Time, Days	**Oil Volume, mL**	**Oil Recovery, %**

Table 0.3 Spontaneous Imbibition Data for Core #4

Time, Days	Oil Volume, mL	Oil Recovery, %
0.00	0.0	0.00
0.08	3.0	8.63
0.23	4.0	11.51
1.25	6.9	19.86
2.25	8.0	23.02
3.25	8.9	25.61
4.25	9.5	27.34
5.25	9.8	28.20
6.25	9.9	28.49
7.33	10.2	29.35
8.33	10.3	29.64
9.33	10.3	29.64
10.33	10.2	29.35
11.33	10.3	29.64
12.33	10.3	29.64
13.33	10.3	29.64
14.33	10.3	29.64
14.50	11.1	31.94
15.50	14.7	42.30
16.50	16.2	46.62
17.50	16.3	46.91
18.50	16.4	47.20
19.50	16.5	47.48
20.50	17.7	50.94
21.50	18.5	53.24
22.50	18.6	53.53
23.50	18.6	53.53
24.50	18.7	53.81
25.50	18.7	53.82
Time, Days	**Oil Volume, mL**	**Oil Recovery, %**

Table 0.4 Spontaneous Imbibition Data for Core #6

Time, Days	Oil Volume, mL	Oil Recovery, %
0.00	0.0	0.00
0.04	2.6	7.52
0.25	6.3	18.23
1.25	9.5	27.49
2.25	10.3	29.80
3.21	10.4	30.10
4.21	10.4	30.10
5.21	10.5	30.38
6.21	10.6	30.67
7.21	10.6	30.67
8.21	10.6	30.67
9.21	10.6	30.67
10.21	10.6	30.67
11.21	10.6	30.67
12.21	10.6	30.67
13.21	10.6	30.67
14.00	10.6	30.67
14.04	10.6	30.67
14.29	10.6	30.67
15.29	12.0	34.72
16.29	13.5	39.06
17.29	14.4	41.66
18.29	14.8	42.82
19.29	15.5	44.85
20.29	15.7	45.43
21.29	15.9	46.01
22.29	16.2	46.88
23.29	16.5	47.74
24.29	16.6	48.03
25.29	16.7	48.32
26.29	17.0	49.19

27.29	17.6	50.93
28.29	18.4	53.24
29.29	18.9	54.69
30.29	18.9	54.69
31.29	19.0	54.98
32.29	19.0	54.98
Time, Days	**Oil Volume, mL**	**Oil Recovery, %**

Core Cleaning Data

Table 0.5 Core Cleaning Data for Core #1

PV of DI Flooded	$[SO_4^{-2}]$	$[Ca^{+2}]$	$[Mg^{+2}]$	$[K^+]$	$[Na^+]$	$[Cl^-]$
0.5	0.514885	0.725449	0.152282	0.105360	1.902213	1.663671
1.0	0.631663	0.569839	0.085589	0.210719	2.188085	1.793518
1.5	0.580705	0.36382	0.047797	0.052680	0.722770	0.436206
2.0	0.332286	0.190677	0.032235	0.116812	0.825251	0.580256
2.5	0.170921	0.075613	0.042239	0.048099	0.458473	0.202887
3.0	0.169859	0.135885	0.034458	0.153459	1.046397	0.809518
3.5	0.043526	0.051505	0.010004	0.027485	0.266094	0.097386
4.0	0.054143	0.067942	0.014451	0.151263	1.921991	1.756999
4.5	0.033972	0.033971	0.006669	0.084746	0.668831	0.227233
5.0	0.023272	0.023171	0.004549	0.135135	2.216851	4.455392

Table 0.6 Core Cleaning Data for Core #2

PV of DI Flooded	$[SO_4^{-2}]$	$[Ca^{+2}]$	$[Mg^{+2}]$	$[K^+]$	$[Na^+]$	$[Cl^-]$
0.5	0.365197	0.574222	0.082255	0.018323	0.595116	0.306359
1.0	0.489406	0.440529	0.056689	0.059551	0.713780	0.271868
1.5	0.539302	0.349574	0.04335	0.038937	0.569945	0.257666
2.0	0.320609	0.188485	0.023343	0.004581	0.307447	0.129847
2.5	0.158181	0.075613	0.038904	0.087036	0.706588	0.521419
3.0	0.055204	0.056984	0.014450	0.020614	0.350597	0.176511
3.5	0.035033	0.052601	0.010004	0.032066	0.463867	0.227233
4.0	0.027602	0.069038	0.010004	0.022904	0.420716	0.310417
4.5	0.026540	0.044930	0.007781	0.018323	0.404535	0.282013
5.0	0.038218	0.051505	0.005558	0.029776	0.604106	0.417947

Table 0.7 Core Cleaning Data for Core #4

PV of DI Flooded	$[SO_4^{-2}]$	$[Ca^{+2}]$	$[Mg^{+2}]$	$[K^+]$	$[Na^+]$	$[Cl^-]$
0.5	0.321670	0.36382	0.104486	0.059551	0.517805	0.344907
1.0	0.450126	0.324370	0.060024	0.057261	0.474654	0.231291
1.5	0.423586	0.299165	0.038904	0.043518	0.219348	0.148107
2.0	0.236741	0.149035	0.017785	0.013743	0.246317	0.071010
2.5	0.143318	0.111776	0.014450	0.020614	0.280478	0.142021
3.0	0.076437	0.077805	0.011116	0.020614	0.273286	0.121732
3.5	0.040341	0.058080	0.007781	0.018323	0.321830	0.107530
4.0	0.028664	0.058080	0.007781	0.018323	0.291265	0.133905
4.5	0.027602	0.049313	0.006669	0.006871	0.244519	0.099414
5.0	0.014863	0.051505	0.006669	0.006871	0.257105	0.095357

Table 0.8 Core Cleaning Data for Core #6

PV of DI Flooded	$[SO_4^{-2}]$	$[Ca^{+2}]$	$[Mg^{+2}]$	$[K^+]$	$[Na^+]$	$[Cl^-]$
0.5	0.322732	1.094748	0.244541	0.036647	0.818060	0.902846
1.0	0.449064	0.593948	0.105597	0.041228	0.827050	0.501130
1.5	0.528686	0.415325	0.063358	0.038937	0.309245	0.243464
2.0	0.271774	0.234511	0.03557	0.020614	0.235530	0.186656
2.5	0.128456	0.132597	0.016673	0.011452	0.115068	0.105501
3.0	0.061574	0.059176	0.008892	0.009162	0.347001	0.109559
3.5	0.039280	0.044930	0.005558	0.020614	0.352395	0.164338
4.0	0.059451	0.070134	0.013339	0.006871	0.237327	0.125790
4.5	0.032910	0.044930	0.012227	0.004581	0.285871	0.095357
5.0	0.029725	0.062463	0.010004	0.052680	0.544774	0.486928

Bibliography

1) Al-Maamari, R. S. H., & Buckley, J. S. (2013). Asphaltene Precipitation and Alteration of Wetting: The Potential for Wettability Changes During Oil Production. *SPE reservoir evaluation & engineering*, *6*(4), 210-214. https://doi.org/10.2118/84938-pa

2) Alvarez, J. M., & Sawatzky, R. P. (2013, 2013/6/11/). *Waterflooding: Same Old, Same Old?* SPE Heavy Oil Conference-Canada, Calgary, Alberta, Canada. https://doi.org/10.2118/165406-MS

3) Amott, E. (1959). Observations Relating to the Wettability of Porous Rock. *Transactions of the AIME*, *216*(01), 156-162. https://doi.org/10.2118/1167-G

4) Anderson, W. G. (1986). Wettability Literature Survey- Part 1: Rock/Oil/Brine Interactions and the Effects of Core Handling on Wettability. *Journal of Petroleum Technology*, *38*(10), 1125-1144. https://doi.org/10.2118/13932-PA

5) Anderson, W. G. (2013). Wettability Literature Survey- Part 1: Rock/Oil/Brine Interactions and the Effects of Core Handling on Wettability. *Journal of petroleum technology*, *38*(10), 1125-1144. https://doi.org/10.2118/13932-pa

6) Andreassen, E., Strand, S., Puntervold, T., & Torrijos, I. D. P. (2019). Production of Smart Water by Acid Flooding in Chalk: Temperature Limitation at Slightly Water-Wet Conditions. In: University of Stavanger, Norway.

7) Buckley, J. S. (1996). *Mechanisms and consequences of wettability alteration by crude oils* Department of Petroleum Engineering, Heriot-Watt University]. Edinburgh.

8) Buckley, J. S., & Liu, Y. (1998). Some mechanisms of crude oil/brine/solid interactions. *Journal of Petroleum Science and Engineering*, *20*(3), 155-160. https://doi.org/https://doi.org/10.1016/S0920-4105(98)00015-1

9) Buckley, J. S., Takamura, K., & Morrow, N. R. (2013). Influence of Electrical Surface Charges on the Wetting Properties of Crude Oils. *SPE reservoir engineering*, *4*(3), 332-340. https://doi.org/10.2118/16964-pa

10) Chilingar, G. V., & Yen, T. F. (1983). Some Notes on Wettability and Relative Permeabilities of Carbonate Reservoir Rocks, II. *Energy Sources*, *7*(1), 67-75. https://doi.org/10.1080/00908318308908076

11) Cook, T. A. (2013). *Reserve growth of oil and gas fields—Investigations and applications* (2013-5063). (Scientific Investigations Report, Issue. U. S. G. Survey. http://pubs.er.usgs.gov/publication/sir20135063

12) Craig, F. F. (1971). *The reservoir engineering aspects of waterflooding* (Vol. vol. 3). Henry L. Doherty Memorial Fund of AIME.

13) Cuiec, L. (1984, 1984/1/1/). *Rock/Crude-Oil Interactions and Wettability: An Attempt To Understand Their Interrelation* SPE Annual Technical Conference and Exhibition, Houston, Texas. https://doi.org/10.2118/13211-MS

14) Denekas, M. O., Mattax, C. C., & Davis, G. T. (1959). Effects of Crude Oil Components on Rock Wettability. *Transactions of the AIME, 216*(01), 330-333. https://doi.org/10.2118/1276-G

15) Fathi, S., Austad, T., & Strand, S. (2011). Water-Based Enhanced Oil Recovery (EOR) by "Smart Water": Optimal Ionic Composition for EOR in Carbonates. *Energy & Fuels, 25*, 5173–5179. https://doi.org/10.1021/ef201019k

16) Fathi, S., Austad, T., & Strand, S. (2012). Water-Based Enhanced Oil recovery (EOR) by "Smart Water" in Carbonate Reservoirs. https://doi.org/10.2118/154570-MS

17) Flügel, E. (2010). *Microfacies of Carbonate Rocks: Analysis, Interpretation and Application* (2. Aufl. ed.). Springer-Verlag.

18) Frykman, P. (2001). Spatial variability in petrophysical properties in Upper Maastrichtian chalk outcrops at Stevns Klint, Denmark. *Mar. Pet. Geol.*, *18*(10), 1041.

19) Green, D. W., & Willhite, G. P. (1998). *Enhanced oil recovery* (Vol. vol. 6). Henry L. Doherty Memorial Fund of AIME, Society of Petroleum Engineers.

20) Hirasaki, G. J. (1991). Wettability: Fundamentals and Surface Forces. *SPE formation evaluation*, *6*(2), 217-226. https://doi.org/10.2118/17367-PA

21) IEA, *Global share of total energy supply by source, 2018*, IEA, Paris https://www.iea.org/data-and-statistics/charts/global-share-of-total-energy-supply-by-source-2018

22) Jadhunandan, P. P., & Morrow, N. R. (2013). Effect of Wettability on Waterflood Recovery for Crude-Oil/Brine/Rock Systems. *SPE reservoir engineering*, *10*(1), 40-46. https://doi.org/10.2118/22597-pa

23) Kovscek, A. R., Wong, H., & Radke, C. J. (1992). A pore-level scenario for the development of mixed-wettability in oil reservoirs. In: Lawrence Berkeley Laboratory.

24) Kowalewski, E., Boassen, T., & Torsæter, O. (2003). Wettability alterations due to aging in crude oil; wettability and Cryo-ESEM analyses. *Journal of Petroleum Science and Engineering - J PET SCI ENGINEERING*, *39*, 377-388. https://doi.org/10.1016/S0920-4105(03)00076-7

25) Letellier, P., Mayaffre, A., & Turmine, M. (2007). Drop size effect on contact angle explained by nonextensive thermodynamics. Young's equation revisited. *Journal of Colloid and Interface Science*, *314*(2), 604-614. https://doi.org/https://doi.org/10.1016/j.jcis.2007.05.085

26) Lindanger, M. (2019). Production of Smart Water by Acid Flooding in Chalk Cores: Oil Recovery Effects at Intermediate Temperature. In: University of Stavanger, Norway.

27) Menezes, J., Yan, J., & Sharma, M. (1989). The Mechanism of Wettability Alteration Due to Surfactants in Oil-Based Muds. https://doi.org/10.2118/18460-MS

28) Moore, T. F., & Slobod, R. L. (1955, 1955/1/1/). *Displacement of Oil by Water-Effect of Wettability, Rate, and Viscosity on Recovery* Fall Meeting of the Petroleum Branch of AIME, New Orleans, Louisiana. https://doi.org/10.2118/502-G

29) Muggeridge, A., Cockin, A., Webb, K., Frampton, H., Collins, I., Moulds, T., & Salino, P. (2014). Recovery rates, enhanced oil recovery and technological limits. *Philos Trans A Math Phys Eng Sci*, *372*(2006), 20120320-20120320. https://doi.org/10.1098/rsta.2012.0320

30) Pierre, A., Lamarche, J. M., Mercier, R., Foissy, A., & Persello, J. (1990). CALCIUM AS POTENTIAL DETERMINING ION IN AQUEOUS CALCITE SUSPENSIONS. *Journal of Dispersion Science and Technology*, *11*(6), 611-635. https://doi.org/10.1080/01932699008943286

31) Puntervold, T., Strand, S., & Austad, T. (2007). New method to prepare outcrop chalk cores for wettability and oil recovery studies at low initial water saturation. *Energy Fuels*, *21*(6), 3425.

32) Puntervold, T. (2008). *Waterflooding of carbonate reservoirs : EOR by wettability alteration* University of Stavanger, Faculty of Science and Technology, Department of Petroleum Engineering]. Stavanger.

33) Puntervold, T., Strand, S., & Austad, T. (2008). Co-injection of seawater and produced water to improve oil recovery from fractured North Sea chalk oil reservoirs. *J. Pet. Sci. Eng.*

34) Røgen, B., & Fabricius, I. L. (2002). Influence of clay and silica on permeability and capillary entry pressure of chalk reservoirs in the North Sea. *Pet. Geosci.*, *8*(3), 287.

35) Standnes, D. C. (2001). *Enhanced oil recovery from oil-wet carbonate rock by spontaneous imbibition of aqueous surfactant solutions* Norges teknisk-naturvitenskapelige universitet, Petroleumsteknologi og anvendt geofysikk]. Trondheim.

36) Standnes, D. C., & Austad, T. (2000). Wettability alteration in chalk. 1. Preparation of core material and oil properties. *J. Pet. Sci. Eng.*, *28*(3), 111.

37) Standnes, D. C., & Austad, T. (2003). Wettability alteration in carbonates: Interaction between cationic surfactant and carboxylates as a key factor in wettability alteration from oil-wet to water-wet conditions. *Colloids and Surfaces A: Physicochemical and Engineering Aspects*, *216*(1), 243-259. https://doi.org/https://doi.org/10.1016/S0927-7757(02)00580-0

38) Strand, S. (2005). *Wettability alteration in chalk : a study of surface chemistry* University of Stavanger. Stavanger.

39) Strand, S., Austad, T., Puntervold, T., Høgnesen, E. J., Olsen, M., & Barstad, S. M. F. (2008). "Smart Water" for Oil Recovery from Fractured Limestone: A Preliminary Study. *Energy & Fuels*, *22*(5), 3126-3133. https://doi.org/10.1021/ef800062n

40) Strand, S., Høgnesen, E. J., & Austad, T. (2006). Wettability alteration of carbonates—Effects of potential determining ions (Ca2+ and SO42−) and temperature. *Colloids and Surfaces A: Physicochemical and Engineering Aspects*, *275*(1), 1-10. https://doi.org/https://doi.org/10.1016/j.colsurfa.2005.10.061

41) Strand, S., Puntervold, T., & Austad, T. (2008). Effect of Temperature on Enhanced Oil Recovery from Mixed-Wet Chalk Cores by Spontaneous Imbibition and Forced Displacement Using Seawater. *Energy & Fuels*, *22*(5), 3222-3225. https://doi.org/10.1021/ef800244v

42) Strand, S., Standnes, D., & Austad, T. (2006). New wettability test for chalk based on chromatographic separation of SCN− and SO4 2−. *Journal of Petroleum Science and*

Engineering - J PET SCI ENGINEERING, *52*, 187-197. https://doi.org/10.1016/j.petrol.2006.03.021

43) Thomas, M. M., Clouse, J. A., & Longo, J. M. (1993). Adsorption of organic compounds on carbonate minerals: 3. Influence on dissolution rates. *Chemical Geology*, *109*(1), 227-237. https://doi.org/https://doi.org/10.1016/0009-2541(93)90072-Q

44) Torrijos, I. D. P., Puntervold, T., & Strand, S. (2017). Enhanced oil recovery from Sandstones and Carbonates with "Smart Water". In: University of Stavanger, Norway.

45) Torsæter, O., & Silseth, J. K. (1985). *The effects of sample shape and boundary conditions on capillary imbibition.*

46) Treiber, L. E., & Owens, W. W. (1972). A Laboratory Evaluation of the Wettability of Fifty Oil-Producing Reservoirs. *Society of Petroleum Engineers journal*, *12*(6), 531-540. https://doi.org/10.2118/3526-PA

47) Wade, J. E. (1971, 1971/1/1/). *Some Practical Aspects of Waterflooding* 8th World Petroleum Congress, Moscow, USSR.

48) Yuan, Y., & Lee, T. R. (2013). Contact Angle and Wetting Properties. In G. Bracco & B. Holst (Eds.), *Surface Science Techniques* (pp. 3-34). Springer Berlin Heidelberg. https://doi.org/10.1007/978-3-642-34243-1_1

49) Zhang, P. (2006). *Water-based EOR in fractured chalk : wettability and chemical additives* University of Stavanger, Faculty of Science and Technology, Department of Petroleum Engineering. Stavanger.

50) Zhang, P., & Austad, T. (2006). *Colloids Surf., A*, *279*, 179.

51) Zhang, P., Tweheyo, M. T., & Austad, T. (2006). *Energy Fuels*, *20*, 2056.

52) Zhang, P., Tweheyo, M. T., & Austad, T. (2007a). *Colloids Surf., A*, *301*, 199.

53) Zhang, P., Tweheyo, M. T., & Austad, T. (2007b). Wettability alteration and improved oil recovery by spontaneous imbibition of seawater into chalk: Impact of the potential determining ions: Ca2+, Mg2+ and SO42−. *Colloids Surf., A*, *301*, 199.

54) Zhou, X., Morrow, N., Of, U., Ma, S., & Research, W. (1996). Interrelationship of Wettability, Initial Water Saturation, Aging Time, and Oil Recovery by Spontaneous Imbibition and Waterflooding. *SPE Journal*, *5*. https://doi.org/10.2118/35436-MS